temperature. Cells were then incubated with a secondary antibody, Texas red–conjugated horse anti-mouse immunoglobulin G (IgG) (Vector, Burlingame, CA) or goat anti-rabbit IgG (Vector) for 30 minutes at room temperature.

Myocardial Infarction and Transplantation

All operations on cynomolgus monkeys were performed under an isoflurane-induced general anesthesia. Thoracotomy was conducted, the pericardium was opened, and the left anterior descending coronary artery was ligated with 5-0 prolene sutures. One to 2 hours after the ligation, GFP-transduced, autologous $CD34^+$ cells in normal saline were injected with a microsyringe through a 27-gauge needle into 10 sites (5 μl/site) in the peri-ischemic zone. In the control group, saline alone was injected in the same way. The pericardium and chest were closed. The animals then received butorphanol tartrate (0.5 mg/kg, intramuscularly) daily for 5 days to alleviate the pain associated with the operation and myocardial infarction.

Echocardiography

Echocardiographic imaging was obtained using a Sonos 5500 system (Philips Medical Systems, Andover, MA) before transplantation and at 2 weeks after transplant. The echocardiography was conducted by independent technicians irrelevant to our study group. In one animal (BM97080), it was additionally performed at 12 weeks. Short-axis two-dimensional images at the midpapillary level of the left ventricle were stored, and percent fractional shortening (%FS) was calculated to assess cardiac function.

Myocardial contrast echocardiography (MCE) was performed at day 0 (just before transplantation) and at 2 weeks after transplant to assess regional blood flow and blood flow defect size. In one animal (BM97080), chronic assessment was performed at 12 weeks after transplant. The electrocardiograph-triggered end-systolic intermittent imaging was conducted in short-axis views at incremental pulsing intervals (triggering intervals of 1, 2, 3, 4, and 8 beats) using an S12 probe. Once optimized, the settings of depth (4 cm), mechanical index (0.9), and focus (3 cm) were fixed. The contrast agent (perflutren; Yamanouchi, Tokyo) consisted of lipid-coated microbubbles of perfluorocarbon [16]. Perflutren diluted with saline (1:10) was administered intravenously at a constant rate (0.01 ml/kg per min). For the assessment of regional blood flow, MCE images were analyzed using ORIGIN 6.0J (Lightstone, Tokyo), and the blood flow was calculated as previously described [17]. Data are presented as a blood flow ratio (the peri-infarct versus nonischemic control region or the infarct versus nonischemic control region). For the assessment of blood flow defect, MCE images obtained at triggering interval of four beats were analyzed using National Institutes of Health Image software (version 1.61). Data are presented as percent defect compared with the total blood flow.

Microspheres

Colored microspheres (15 μm ± 2% diameter; E-Z Trac, Los Angeles) were used to evaluate regional blood flow 2 weeks after transplant [18], with the exception of one animal (BM97080), in which evaluation was performed 12 weeks after transplant. A set of microspheres (2×10^6) was diluted in 2 ml of saline and injected into the left ventricle over 30 seconds. A reference blood sample was withdrawn at a constant rate of 5 ml/min through the femoral artery. After the collection of blood samples, monkeys were irrigated with saline for mercy killing and blood was completely washed out. The heart was excised from each monkey. Tissue samples from the infarct, peri-infarct, and nonischemic regions (one sample per region) were digested, microspheres were collected, and the blood flow was calculated according to the manufacturer's instructions. Data are presented as blood flow ratio (the peri-infarct versus nonischemic control region or the infarct versus nonischemic control region).

Immunohistochemistry

Tissue samples from the infarct, peri-infarct, and nonischemic regions at 2 weeks after transplant were embedded in optimal cutting temperature compound (Sakura, Zoeterwoude, Netherlands) and frozen in liquid nitrogen. Sections were prepared (6 μm), fixed for 10 minutes at 4°C in 4% paraformaldehyde in phosphate-buffered saline (PBS), and blocked with 1% BSA in PBS. The sections were incubated at room temperature with a primary antibody, monoclonal mouse anti-human CD31 (1:200; Becton Dickinson), followed by a secondary antibody, biotin-conjugated horse anti-mouse IgG (1:500; Vector). The sections were then treated with avidin-alkaline phosphatase (ABC AP kit; Vector) for 30 minutes. The reaction was developed with a Vector Red substrate kit (SK-5100; Vector). In the case of double staining of CD31 and GFP, the above sections were further incubated with polyclonal rabbit anti-GFP (1:200; Clontech) followed by biotin-conjugated anti-rabbit IgG (1:500; Vector) and treated with avidin-peroxidase (ABC Elite kit; Vector). The reaction was developed with a Vector SG substrate kit (SK-4700; Vector). The sections were counterstained with hematoxylin, mounted in glycerol, and examined under a light microscope.

In Situ Polymerase Chain Reaction

In situ detection of transduced cell progeny was performed by amplifying proviral sequences as previously reported [19]. The following primer set for the GFP gene was used:

5'-CGT CCA GGA GCG CAC CAT CTT C-3' and 5'-GGT CTT TGC TCA GGG CGG ACT-3'. The polymerase chain reaction (PCR) mixture consisted of 420 μM dATP, 420 μM dCTP, 420 μM dGTP, 378 μM dTTP, 42 μM digoxigenin-labeled dUTP (Roche, Mannheim, Germany), 0.8 μM of each GFP primer, 4.5 mM $MgCl_2$, 1 × PCR buffer (Mg^{2+} free), and 4 U of Takara Taq DNA polymerase (Takara, Kyote). Sections were prepared with a Takara slide frame (Takara) from the infarct, peri-infarct, and nonischemic regions at 2 weeks after transplant. PCR was performed using a PTC100 thermal cycler (MJ Research, Watertown, MA) with the following conditions: 94°C for 1 minute and 57°C for 1 minute with 10 cycles. The digoxigenin-incorporated DNA fragments were detected using horseradish peroxidase (HRP)-conjugated rabbit F(ab') anti-digoxigenin antibody (DakoCytomation). The sections were then stained for HRP using a Vector SG substrate kit (Vector). Finally, the sections were counterstained with a Kernechtrot solution (Muto, Tokyo) that stains nucleotides, mounted in glycerol, and examined under a light microscope.

ELISA

Vascular endothelial growth factor (VEGF) and basic fibroblast growth factor (bFGF) levels in tissue lysate or medium were assessed by ELISA (R&D Systems, Minneapolis) according to the manufacturer's instructions. Tissue lysate was obtained from the peri-infarct region (three samples from each monkey) at 2 weeks after transplant. Briefly, tissue was homogenized and suspended in lysis buffer containing 10 mM Tris-HCl (pH 8.0), 1% Nonidet P-40, 150 mM NaCl, and protease inhibitor cocktail tablets (Complete Mini, Roche). The suspension was rocked at 4°C for 20 minutes and centrifuged at 16,000g and 4°C for 30 minutes. The supernatant was used for ELISA. The protein concentration of lysate was determined with DC Protein Assay (Bio-Rad, Hercules, CA).

Results

Lentiviral Marking

The CD34+ fraction of autologous bone marrow cells was used for transplantation in our study (Table 1). Before transplantation, CD34+ cells were genetically marked with GFP using an SIV-based lentivirus vector. The ex vivo transduction results are summarized in Table 1. The transduced cells were frozen until transplantation. An aliquot of the transduced cells was examined in vitro for the endothelial differentiation ability. After the differentiation culture, a vessel-like structure was observed (Fig. 1A). The ability of cells to take up DiI-acetylated LDL and the expression of CD31, vWF, VE-cadherin, and VEGFR-2 suggested the endothelial lineage (Fig. 1B). We and others have already confirmed the ability of hematopoietic differentiation of the cells [20, 21]. Taken together, the SIV-mediated GFP gene transfer does not spoil the differentiation abilities of CD34+ cells. In addition, on average, 41% of cells fluoresced 48 hours after transduction, and 56% of

Table 1. Summary of ex vivo transduction and transplantation

	Sex	Age (y)	Body weight (kg)	Harvested bone marrow cell number	Isolated CD34+ cell number	Transplanted cell number	% GFP expression Before[a]	% GFP expression After[b]
Saline group								
CTR01061[c]	M	3	4.1			NA		
CTR99056	M	3	3.4					
CTR96116	F	5	3.2					
CTR99051	M	5	5.9					
CD34+ cell group								
BM01052	M	3	3.9	213×10^6	1.00×10^6	0.47×10^6	49	87
BM01051[d]	M	3	4.1	396×10^6	5.14×10^6	2.20×10^6	51	54
BM97080[e]	M	5	3.9	330×10^6	2.35×10^6	1.04×10^6	49	67
BM90047	M	13	5.8	343×10^6	3.10×10^6	1.07×10^6	16	14
Average		5	4.3	321×10^6	2.90×10^6	1.20×10^6	41	56

[a]Before endothelial differentiation of GFP-transduced CD34+ cells.
[b]After the in vitro endothelial differentiation.
[c]CTR01061 died of heart failure 5 days after myocardial infarction.
[d]BM01051 developed a ventricular aneurysm after myocardial infarction.
[e]BM97080 was killed 12 weeks after the treatment. All other animals were killed 2 weeks after the treatment.
Abbreviations: GFP, green fluorescent protein; NA, not applicable.

endothelial cells still fluoresced after in vitro differentiation (Table 1), showing that the GFP expression is stable during the in vitro differentiation to endothelial cells. Thus, GFP was expected to serve as a good genetic tag after transplantation.

Acute Myocardial Infarction and Autologous Transplantation

Cynomolgus acute myocardial infarction was generated by ligating the left anterior descending artery. One to two hours after the ligation, GFP-transduced, autologous CD34$^+$ cells were injected in the peri-ischemic zone at 10 sites (total, $1.20 \pm 0.73 \times 10^6$ cells; $n = 4$). In the control group, saline was injected in the same way ($n = 4$). We conducted contrast echocardiography immediately after the coronary ligation and found no significant differences in the blood flow defect size (percent blood flow defect compared with the total) between the cell-treated and saline-treated groups ($13.0 \pm 2.1\%$ versus $12.3 \pm 3.5\%$, $p = .75$), suggesting that the initial risk of infarction did not differ between the two groups. In addition, we tried to assess the cardiac isozyme of serum creatine kinase (CK) to evaluate the infarct size; however, either the immuno-inhibition assay or chemical luminescence immunoassay did not work well for cynomolgus monkey samples. We were at least able to show that total CK values at 24 hours after the ligation did not significantly differ between the two groups ($p = .83$).

One of the control monkeys (CTR01061) died of heart failure 5 days after myocardial infarction, and the other control monkeys showed a decrease in %FS at 2 weeks after infarction (Fig. 2). Thus, all four control animals showed the deteriorated cardiac function. In the cell-treated group, one monkey (*, BM01051) underwent ventricular fibrillation immediately after the ligation and survived after cardiopulmonary resuscitation but eventually developed a ventricular aneurysm. Only this animal showed a decrease in %FS despite CD34$^+$ cell treatment; the other animals receiving CD34$^+$ cells showed an increase in %FS (Fig. 2). CD34$^+$ cell treatment may not be able to rescue such a heavily impaired heart but otherwise had a significant effect on cardiac function. Even an old monkey (BM90047, Table 1) showed improved %FS.

The relative blood flow in the peri-infarct to nonischemic control region was also significantly ameliorated in the CD34$^+$ cell–treated monkeys compared with the saline-treated ones, as assessed using contrast echocardiography (Fig. 3A) and colored microspheres (Fig. 3B). An excellent correlation was found between the two methods (Fig. 3C; correlation coefficient = 0.93). Two groups (CD34$^+$ cell–treated and saline-treated) were well separated on the panel, showing an obvious positive effect of CD34$^+$ cell injection on the blood flow in the peri-infarct zone after acute myocardial infarction. In fact, the average myocardial blood flow in the peri-infarct region in the absolute value was 0.988 ml/g per minute and 0.383 ml/g per minute for the cell-treated and saline-treated groups, respectively. Of note, the blood flow in the peri-infarct zone was ameliorated even in the animal with a ventricular aneurysm. On the other hand, the relative blood flow in the infarct to nonischemic region did not show

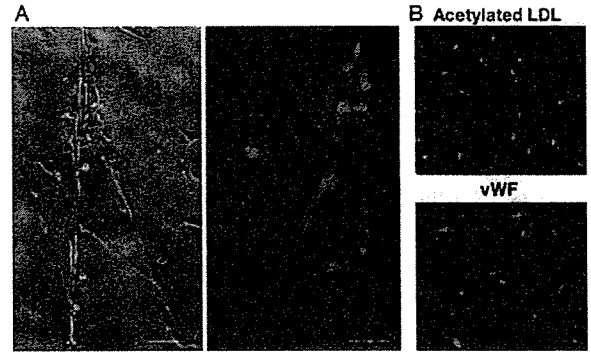

Figure 1. In vitro endothelial differentiation of cynomolgus CD34$^+$ cells lentivirally transduced with GFP. The transduced CD34$^+$ cells were differentiated to endothelial cells after 7 days in culture. **(A)**: Representative vessel-like structure derived from CD34$^+$ cells observed under a phase-contrast microscope (left) and a fluorescent microscope (right). **(B)**: The transduced CD34$^+$ cells differentiated into fluorescent cells (green) positive for the cellular intake of acetylated LDL and immunostaining for von Willebrand factor (vWF) (stained in red). Bar = 100 μm. Abbreviations: GFP, green fluorescent protein; LDL, low-density lipoprotein.

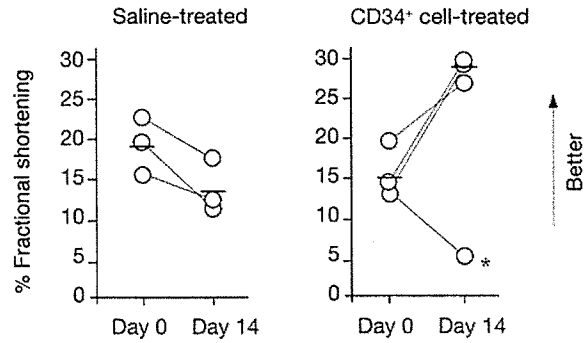

Figure 2. Improved cardiac function after CD34$^+$ cell transplantation. Cardiac function was assessed by echocardiography in terms of percent fractional shortening (%FS) before and 2 weeks after treatment. One monkey in the saline-treated group (CTR01061) died of heart failure 5 days after myocardial infarction and is not included in the figure. One monkey in the CD34$^+$ cell–treated group (*, BM01051) developed a left ventricular aneurysm after myocardial infarction. If this animal was excluded from the statistical analysis, the cardiac function was significantly improved in the CD34$^+$ cell–treated compared with the saline-treated group in terms of the ratio of %FS at day 14 versus day 0 after transplant ($p = .017$).

a significant difference between the CD34+ cell–treated and saline-treated groups. The peri-infarct region was the injection site, and thus the highest degree of change would be expected there.

All monkeys except one CD34+ cell–treated monkey (BM97080) were examined for cardiac function and blood flow at 2 weeks after transplantation, and their tissue sections were finally prepared at this time point (see below). BM97080 was examined at 12 weeks, at which time the cardiac function was still improved compared with immediately after infarction (data not shown) and the blood flow data were in a position similar to the cell-treated group at 2 weeks (Fig. 3C).

In Vivo Tracking of Transplanted Cells

Two weeks after the transplantation, tissue sections were prepared from the infarct, peri-infarct, and nonischemic regions. Immunostaining of an endothelial marker CD31 demonstrated more vessels in the peri-infarct region of the CD34+ cell-treated than saline-treated myocardium (Fig. 4A). In fact, the capillary density of the peri-infarct region was significantly better preserved in the cell-treated than saline-treated group, although there was no significant difference in the capillary density of the nonischemic control regions between the two groups (Fig. 4B).

Double immunostaining with anti-CD31 and anti-GFP showed that some cells in vessels were positive for both CD31 and GFP in the peri-infarct region (Fig. 5A). The result clearly indicates that at least some transplanted CD34+ cells gave rise to endothelial cells. However, we found that the transplanted cell progeny accounted for only a small fraction of endothelial cells after examining more than 100 sections of the peri-infarct region. In situ PCR for proviral GFP sequences also showed that few CD31-positive endothelial cells contained the GFP-provirus (Fig. 5B). There were no GFP-positive cardiomyocytes in more than 100 sections. Most of the transplanted cell progeny were found not incorporated in vessels (Fig. 5C). Hematoxylin-eosin staining did not show any noncardiac tissue regeneration in the myocardium.

On the other hand, we found that in vitro conditioned medium of CD34+ cell culture for endothelial differentiation contained high levels of VEGF, whereas unconditioned medium did not contain detectable VEGF, as assessed

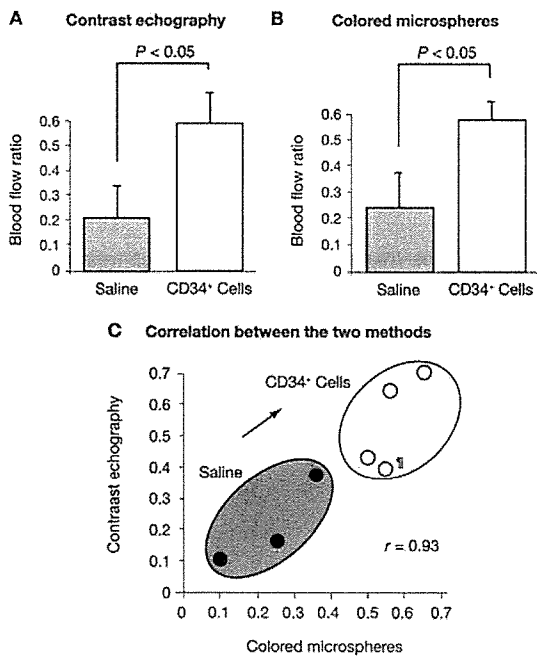

Figure 3. Improved regional blood flow after CD34+ cell transplantation. Myocardial contrast echocardiography (**A**) and colored microspheres (**B**) showed a significantly ameliorated blood flow ratio (the peri-infarct to nonischemic control region) in the CD34+ cell–treated monkeys ($n = 3$) compared with the saline-treated monkeys ($n = 3$) at 2 weeks after treatment. (**C**): An excellent correlation was found between the two methods. A CD34+ cell–treated monkey (¶, BM97080) that was examined at 12 weeks after transplant is included in the panel (**C**) but excluded from the statistical analysis in (**A**) and (**B**).

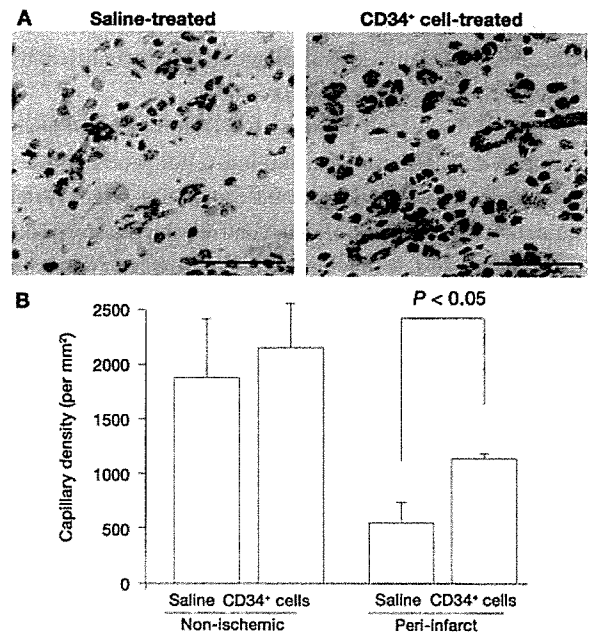

Figure 4. Neoangiogenesis in the ischemic myocardium. Tissue sections were prepared at 2 weeks after the treatment. (**A**): Representative results of immunostaining with anti-CD31 (stained in brown) in the peri-infarct region of the saline-treated and CD34+ cell–treated myocardium. Bar = 50 μm. (**B**): The density of CD31-positive capillaries in the peri-infarct and control nonischemic regions in the saline-treated and CD34+ cell–treated groups. Five fields for each section were randomly selected ($n = 3$ for the saline injection, $n = 3$ for the CD34+ cell injection), and the number of CD31-positive capillaries was counted (average ± standard deviation).

by ELISA (Fig. 6A). In addition, in vivo VEGF levels in the peri-infarct tissue were significantly higher in the CD34$^+$ cell–treated than saline-treated group (Fig. 6B, left), although in vivo levels of bFGF differed little between the two groups (Fig. 6B, right).

Discussion

Although gained with small numbers of cynomolgus monkeys, our data suggest that the direct transplantation of bone marrow CD34$^+$ cells, even without coronary bypass grafts or percutaneous coronary intervention, results in improved regional blood flow and cardiac function after myocardial infarction in nonhuman primates. Furthermore, we have tried to see the contribution of transplanted CD34$^+$ cells to the repair of ischemic myocardium. To this end, we genetically marked CD34$^+$ cells with GFP using an SIV-based lentiviral vector before transplantation. Lentiviral vectors can transduce nondividing cells unlike oncoretroviral vectors, and thus the ex vivo culture period with multiple cytokines to allow cell cycling can be reduced to 1 day or less [20, 22, 23]. This is the great advantage of using lentiviral vectors over oncoretroviral vectors for transduction of multipotent stem cells, given that extended ex vivo culture of stem cells may result in loss of multilineage differentiation and engraftment abilities [24]. Human immunodeficiency virus (HIV)-1–based lentiviral vectors can efficiently transduce human cells, but not Old World monkey cells [25]. According to a recent report, a species-specific cytoplasmic component confers the innate

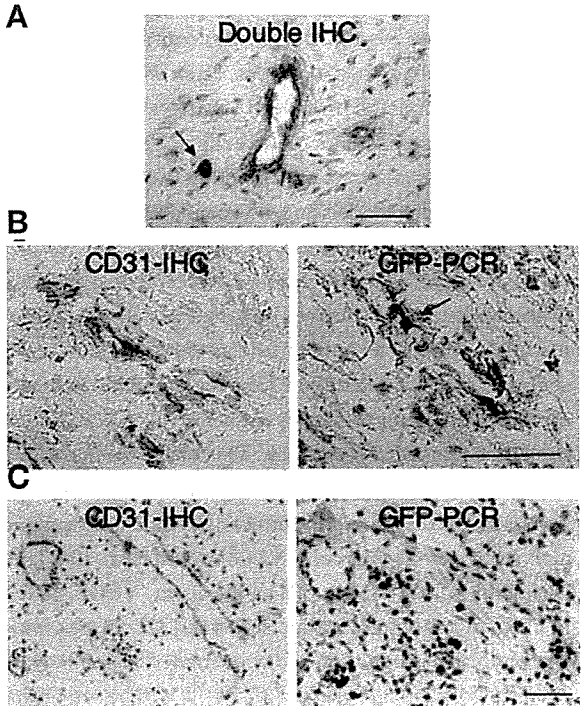

Figure 5. In vivo fate of transplanted cells. Cardiac sections were prepared at 2 weeks after transplantation. **(A)**: Double immunohistochemistry (IHC) with anti-CD31 and anti–green fluorescent protein (GFP) in the peri-infarct region of the CD34$^+$ cell–treated myocardium. Some cells (arrow) were positive for both CD31 (stained in brown) and GFP (stained in black), but such cells were rare. **(B, C)**: Serial sections from the peri-infarct region of the CD34$^+$ cell–treated myocardium. One section (left) was stained with anti-CD31 (stained in brown), and the other (right) was assessed by in situ polymerase chain reaction (PCR) for proviral GFP sequences (stained in black). **(B)**: Some CD31-positive endothelial cells contained the GFP-provirus (arrow, right panel), but such cells were rare. **(C)**: Transplanted cell progeny (cells positive for GFP-provirus in the right panel) were not incorporated in vessels (cells positive for CD31 in the left panel). Bar = 50 μm.

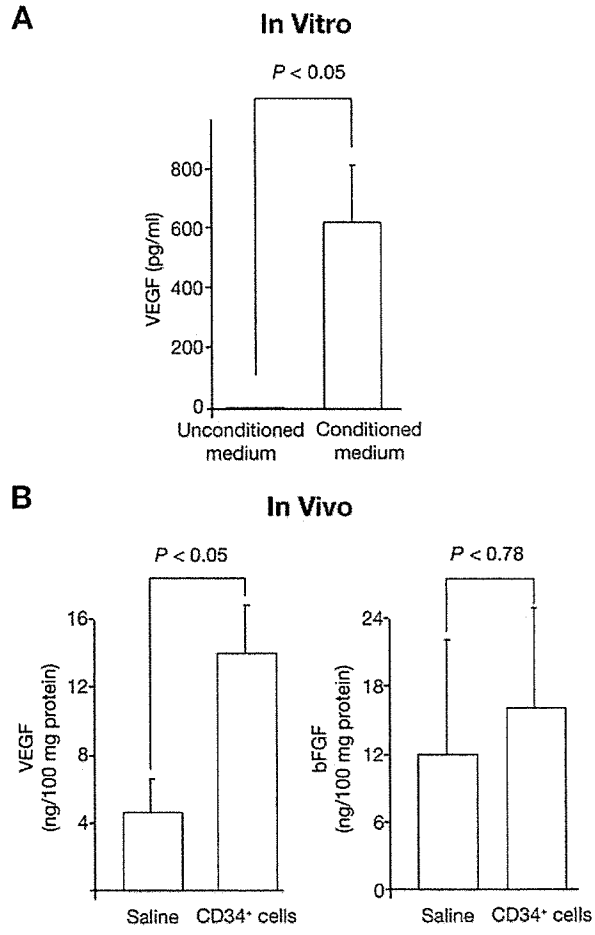

Figure 6. VEGF is implicated in the neoangiogenesis. **(A)**: Unconditioned and conditioned media of in vitro CD34$^+$ cell cultures for endothelial differentiation were examined for VEGF by ELISA. The average ± standard error of six culture dishes is shown. **(B)**: Lysates (three samples per monkey) from the peri-infarct region of the CD34$^+$ cell–treated (monkey, n = 3) and saline-treated (monkey, n = 3) myocardium were prepared and examined for VEGF and basic fibroblast growth factor (bFGF) by ELISA. Data are shown as the average ± standard error. Abbreviation: VEGF, vascular endothelial growth factor.

postentry restriction to HIV-1 infection in simian cells [26]. Unlike HIV-1–based lentiviral vectors, SIV-based ones can efficiently transduce simian hematopoietic stem/progenitor cells [21]. In this study, we also used an SIV-based lentiviral vector and achieved the efficient gene transfer into simian CD34+ cells.

As a result of this marking study, we found only a few GFP-positive cells incorporated into the vascular structure in the ischemic myocardium at 2 weeks after transplantation. GFP-positive cardiomyocytes were not detectable. The existence of GFP-positive endothelial cells can be explained by fusion events [27, 28]. However, if that is the case, GFP-positive cardiomyocytes should have also been detected, given that cardiomyocytes are even easier targets of fusion than endothelial cells [11, 29]. Whether fusion occurred or not, only a few transplanted cells gave rise to nonhematopoietic cells in our primate model.

There are several possible explanations for the very low prevalence of transplanted cell–derived endothelial cells or cardiomyocytes in the ischemic myocardium. First, 2 weeks was too short or the number of transplanted cells was too small to see the nonhematopoietic differentiation. However, the cardiac function and regional blood flow were ameliorated by this time point and with this number of transplanted cells. Thus, if transplanted cell–derived, nonhematopoietic differentiation was a reason for the improvement, transplanted cells at this number should have given rise to such cells by this time point. In fact, Orlic et al. [8] observed transplanted cell-derived endothelial cells and cardiomyocytes within 11 days after transplant in mice. In addition, we observed the endothelial differentiation from CD34+ cells within 7 days in vitro (Fig. 1). However, we cannot formally rule out a possibility that inflammatory responses after generation of infarction might have negative effects on engraftment of transplanted cells. Second, the SIV vector failed to transduce stem or progenitor cells that might be responsible for nonhematopoietic differentiation. Even if the transduction was successful, the cytokine treatment during the transduction or GFP expression in the cells spoiled the differentiation abilities. However, we have shown that the SIV vector successfully transduced cells that were capable of differentiating into GFP-expressing endothelial cells (Fig. 1). We have not examined the differentiation ability to cardiomyocytes, because the method to differentiate CD34+ cells to cardiomyocytes in vitro has not been well established. Thus, we cannot formally rule out the possibility that the ex vivo culture spoiled the ability to differentiate to cardiomyocytes or reduced the ability to differentiate to endothelial cells. Third, cells expressing xenogeneic GFP were rejected via immune responses. However, 2 weeks is too short to allow immune elimination of GFP-expressing cells in monkeys [30, 31]. Fourth, the GFP expression was shut down because of transcriptional silencing in vivo, resulting in negative immunostaining with anti-GFP. To examine this possibility, we tried to detect the provirus (vector integrated into genome) in the cardiac tissue by in situ PCR and found again that only a few CD31-positive endothelial cells contained the GFP-provirus (Fig. 5B), thus arguing against transcriptional silencing-based negative immunostaining with anti-GFP. Taken together, we concluded that most transplanted cell progeny were not incorporated into the repaired, nonhematopoietic tissues.

Our results are in agreement with recent reports that transplanted hematopoietic cells are unable to transdifferentiate into nonhematopoietic cells in ischemic myocardium in mice [9–11]. Our studies confirm and extend these findings in a couple of ways. First, we show that the cardiac function can be indeed significantly improved after injection of hematopoietic cells in a nonhuman primate model, although the above studies used murine myocardial infarction models and did not address the potential beneficial effects of hematopoietic cell injection. Second, the improvement is unlikely to be the result of generation of transplanted cell–derived endothelial cells or cardiomyocytes. Finally, we have found that cultured CD34+ cells secrete VEGF and that the CD34+ cell–treated myocardium contains a significantly higher level of VEGF than the saline-treated myocardium. This observation raises a possibility that some angiogenic cytokines secreted from transplanted cells (paracrine effects) potentiate angiogenic activity of endogenous cells. VEGF would be a candidate. Despite this, the delivery of a single agent (VEGF) failed in clinical trials for cardiac ischemia [32]. In situ multiple cytokine production and coordinated action may be essential for clinical benefits [33, 34]. It will be important to explore and identify cytokines responsible for the paracrine effect. If transplanted cells serve as cytokine factories rather than stem cells in ischemic tissues, it is not surprising that not only stem cells but other types of cells may also work [35]. The concept of stem cell therapeutics for ischemic diseases needs additional consideration.

ACKNOWLEDGMENTS

The SIV vector was supplied by DNAVEC Corporation (Ibaraki, Japan), and thrombopoietin was supplied by Kirin Brewery Co. Ltd. (Tokyo). We thank Masahiro Shakudo (Sumiyoshi Hospital, Osaka) for analyzing the contrast echocardiography and Yasuhiro Ochiai (Jichi Medical School) for preparing tissue sections.

References

1 Assmus B, Schachinger V, Teupe C et al. Transplantation of progenitor cells and regeneration enhancement in acute myocardial infarction (TOPCARE-AMI). Circulation 2002;106:3009–3017.

2 Strauer BE, Brehm M, Zeus T et al. Repair of infarcted myocardium by autologous intracoronary mononuclear bone marrow cell transplantation in humans. Circulation 2002;106:1913–1918.

3 Tse HF, Kwong YL, Chan JK et al. Angiogenesis in ischaemic myocardium by intramyocardial autologous bone marrow mononuclear cell implantation. Lancet 2003;361:47–49.

4 Perin EC, Dohmann HF, Borojevic R et al. Transendocardial, autologous bone marrow cell transplantation for severe, chronic ischemic heart failure. Circulation 2003;107:2294–2302.

5 Stamm C, Westphal B, Kleine HD et al. Autologous bone-marrow stem-cell transplantation for myocardial regeneration. Lancet 2003;361:45–46.

6 Wollert KC, Meyer GP, Lotz J et al. Intracoronary autologous bone-marrow cell transfer after myocardial infarction: the BOOST randomised controlled clinical trial. Lancet 2004;364:141-148.

7 Asahara T, Murohara T, Sullivan A et al. Isolation of putative progenitor endothelial cells for angiogenesis. Science 1997;275:964–967.

8 Orlic D, Kajstura J, Chimenti S et al. Bone marrow cells regenerate infarcted myocardium. Nature 2001;410:701–705.

9 Murry CE, Soonpaa MH, Reinecke H et al. Haematopoietic stem cells do not transdifferentiate into cardiac myocytes in myocardial infarcts. Nature 2004;428:664–668.

10 Balsam LB, Wagers AJ, Christensen JL et al. Haematopoietic stem cells adopt mature haematopoietic fates in ischaemic myocardium. Nature 2004;428:668–673.

11 Nygren JM, Jovinge S, Breitbach M et al. Bone marrow-derived hematopoietic cells generate cardiomyocytes at a low frequency through cell fusion, but not transdifferentiation. Nat Med 2004;10:494–501.

12 Hanazono Y, Terao K, Ozawa K. Gene transfer into nonhuman primate hematopoietic stem cells: implications for gene therapy. STEM CELLS 2001;19:12–23.

13 Shibata H, Hanazono Y, Ageyama N et al. Collection and analysis of hematopoietic progenitor cells from cynomolgus macaques (Macaca fascicularis): assessment of cross-reacting monoclonal antibodies. Am J Primatol 2003;61:3–12.

14 Nakajima T, Nakamaru K, Ido E et al. Development of novel simian immunodeficiency virus vectors carrying a dual gene expression system. Hum Gene Ther 2000;11:1863–1874.

15 VandenDriessche T, Thorrez L, Naldini L et al. Lentiviral vectors containing the human immunodeficiency virus type-1 central polypurine tract can efficiently transduce nondividing hepatocytes and antigen-presenting cells in vivo. Blood 2002;100:813–822.

16 Kobayashi N, Yasu T, Yamada S et al. Influence of contrast ultrasonography with perflutren lipid microspheres on microvessel injury. Circ J 2003;67:630–636.

17 Wei K, Jayaweera AR, Firoozan S et al. Quantification of myocardial blood flow with ultrasound-induced destruction of microbubbles administered as a constant venous infusion. Circulation 1998;97:473–483.

18 Hale SL, Alker KJ, Kloner RA. Evaluation of nonradioactive, colored microspheres for measurement of regional myocardial blood flow in dogs. Circulation 1988;78:428–434.

19 Haase AT, Retzel EF, Staskus KA. Amplification and detection of lentiviral DNA inside cells. Proc Natl Acad Sci U S A 1990;87:4971–4975.

20 Hanazono Y, Asano T, Ueda Y et al. Genetic manipulation of primate embryonic and hematopoietic stem cells with simian lentivirus vectors. Trends Cardiovasc Med 2003;13:106–110.

21 Hanawa H, Hematti P, Keyvanfar K et al. Efficient gene transfer into rhesus repopulating hematopoietic stem cells using a simian immunodeficiency virus-based lentiviral vector system. Blood 2004;103:4062–4069.

22 Miyoshi H, Smith KA, Mosier DE et al. Transduction of human $CD34^+$ cells that mediate long-term engraftment of NOD/SCID mice by HIV vectors. Science 1999;283:682–686.

23 Horn PA, Keyser KA, Peterson LJ et al. Efficient lentiviral gene transfer to canine repopulating cells using an overnight transduction protocol. Blood 2004;103:3710–3716.

24 Dunbar CE, Takatoku M, Donahue RE. The impact of ex vivo cytokine stimulation on engraftment of primitive hematopoietic cells in a non-human primate model. Ann N Y Acad Sci 2001;938:236–245.

25 Owens CM, Yang PC, Gottlinger H et al. Human and simian immunodeficiency virus capsid proteins are major viral determinants of early, postentry replication blocks in simian cells. J Virol 2003;77:726–731.

26 Stremlau M, Owens CM, Perron MJ et al. The cytoplasmic body component TRIM5α restricts HIV-1 infection in Old World monkeys. Nature 2004;427:848–853.

27 Terada N, Hamazaki T, Oka M et al. Bone marrow cells adopt the phenotype of other cells by spontaneous cell fusion. Nature 2002;416:542–545.

28 Ying QL, Nichols J, Evans EP et al. Changing potency by spontaneous fusion. Nature 2002;416:545–548.

29 Alvarez-Dolado M, Pardal R, Garcia-Verdugo JM et al. Fusion of bone-marrow-derived cells with Purkinje neurons, cardiomyocytes and hepatocytes. Nature 2003;425:968–973.

30 Rosenzweig M, Connole M, Glickman R et al. Induction of cytotoxic T lymphocyte and antibody responses to

enhanced green fluorescent protein following transplantation of transduced CD34(+) hematopoietic cells. Blood 2001;97:1951–1959.

31 Heim DA, Hanazono Y, Giri N et al. Introduction of a xenogeneic gene via hematopoietic stem cells leads to specific tolerance in a rhesus monkey model. Mol Ther 2000;1:533–544.

32 Henry TD, Annex BH, McKendall GR et al. The VIVA trial: vascular endothelial growth factor in ischemia for vascular angiogenesis. Circulation 2003;107:1359–1365.

33 Cao R, Brakenhielm E, Pawliuk R et al. Angiogenic synergism, vascular stability and improvement of hind-limb ischemia by a combination of PDGF-BB and FGF-2. Nat Med 2003;9:604–613.

34 Ziegelhoeffer T, Fernandez B, Kostin S et al. Bone marrow-derived cells do not incorporate into the adult growing vasculature. Circ Res 2004;94:230–238.

35 Kinnaird T, Stabile E, Burnett MS et al. Local delivery of marrow-derived stromal cells augments collateral perfusion through paracrine mechanisms. Circulation 2004;109:1543–1549.

TEF, an antiapoptotic bZIP transcription factor related to the oncogenic E2A-HLF chimera, inhibits cell growth by down-regulating expression of the common β chain of cytokine receptors

Takeshi Inukai, Toshiya Inaba, Jinjun Dang, Ryoko Kuribara, Keiya Ozawa, Atsushi Miyajima, Wenshu Wu, A. Thomas Look, Yojiro Arinobu, Hiromi Iwasaki, Koichi Akashi, Keiko Kagami, Kumiko Goi, Kanji Sugita, and Shinpei Nakazawa

Gain and/or loss of function mediated by chimeric transcription factors generated by nonrandom translocations in leukemia is a key to understanding oncogenesis. E2A–hepatic leukemia factor (HLF), a chimeric basic region/leucine zipper (bZIP) transcription factor expressed in t(17;19)–positive leukemia cells, contributes to leukemogenesis through its potential to inhibit apoptosis. To identify physiologic counterparts of this chimera, we investigated the function of other bZIP factors that bind to the same DNA sequence recognized by E2A-HLF. Here, we show that thyrotroph embryonic factor (TEF), which shares a high level of sequence identity with HLF and recognizes the same DNA sequence, is expressed in a small fraction of each subset of hematolymphoid progenitors. When TEF was introduced into FL5.12 interleukin 3 (IL-3)–dependent cells, TEF protected the cells from apoptosis due to IL-3 deprivation. Unexpectedly, TEF also almost completely down-regulated expression of the common β (βc) chain of cytokine receptors. Consequently, TEF-expressing cells accumulated in G_0/G_1 phase without undergoing apoptosis. These findings suggest that TEF is one of the apoptotic regulators in hematopoietic progenitors and controls hematopoietic-cell proliferation by regulating the expression of the βc chain. In contrast, E2A-HLF promoted cell survival more efficiently than TEF but did not down-regulate βc chain expression, suggesting that E2A-HLF retains ideal properties for driving leukemic transformation. (Blood. 2005;105:4437-4444)

Introduction

Since key systems that regulate cell survival have been conserved through evolution, relatively simple organisms such as *Caenorhabditis elegans* often provide insight into the complex mechanisms that control cell fate in mammals.[1] The genetic approach demonstrated that 2 factors, cell death specification protein 1 (CES-1) and CES-2, regulate the programmed cell death of serotonergic neurosecretory motor (NSM) neurons in *C elegans* in a cell type–specific fashion.[2] Further studies revealed that CES-2 is a transcription factor that belongs to the basic region/leucine zipper (bZIP) superfamily (Figure 1).[3] CES-2 negatively regulates CES-1, a member of the snail family of zinc finger transcription factors,[4] and CES-1 appears to determine the fate of NSM sisters by negatively regulating the expression of *egl1*, a BH3-only proapoptotic member of the B cell lymphoma (Bcl-2) superfamily.[5-7]

Transcription factors that bind to the DNA sequence elements recognized by CES-2 might play important roles in cell type–specific cell death in mammals. The E2A–hepatic leukemia factor (HLF) fusion transcription factor is a good example. This chimera is derived from childhood acute pro-B-cell leukemia harboring a t(17;19) chromosomal translocation.[8-10] It contains the transactivation domains of E2A and the bZIP DNA-binding and dimerization domain of HLF (Figure 1). E2A-HLF promotes the anchorage-independent growth of murine fibroblasts as a homodimer that depends on both the transactivation domain of E2A and the bZIP domain of HLF.[11,12] E2A-HLF induces the expression of annexin II,[13] annexin V, and sushi-repeat protein upregulated in leukemia (SRPUL),[14] which have been postulated to play paraneoplastic roles in coagulopathies and bone invasion, as well as groucho-related genes, and E2A-HLF also suppresses Runt-related 1 (RUNX1).[15] In addition, we and others established transgenic mice expressing *E2AHLF* that develop T-lineage lymphoid malignancies.[16,17] Of note, we demonstrated that E2A-HLF binds avidly to the sequence recognized by CES-2 and protects cells from apoptosis due to growth factor deprivation without promoting cell proliferation.[18-20] The close homology between the bZIP domains of HLF and CES-2 suggests that E2A-HLF subverts a cell-death pathway through a mechanism similar to that used by CES-2 in the worm. Indeed, we have identified SLUG, a zinc finger transcription factor closely related to CES-1, as one of the downstream targets of E2A-HLF in human leukemias associated with the 17;19 translocation and found that SLUG has antiapoptotic potential.[21,22]

These findings suggest that a cell-death pathway in mammalian hematopoietic cells is normally regulated by bZIP factors that exhibit a DNA-binding specificity similar to that of CES-2 or E2A-HLF. HLF is obviously a good candidate for the regulator of apoptosis in hematopoiesis; however, HLF is not expressed in

From the Department of Pediatrics, School of Medicine, University of Yamanashi, Yamanashi, Japan; Department of Molecular Oncology, Research Institute for Radiation Biology and Medicine, Hiroshima University, Hiroshima, Japan; Department of Experimental Oncology, St Jude Children's Research Hospital, Memphis, TN; Division of Hematology, Jichi Medical School, Tochigi, Japan; Institute of Molecular and Cellular Bioscience, the University of Tokyo, Tokyo, Japan; Pediatric Oncology Department and Department of Cancer Immunology & AIDS, Dana-Farber Cancer Institute, Boston, MA.

Submitted August 2, 2004; accepted January 2, 2005. Prepublished online as *Blood* First Edition Paper, January 21, 2005; DOI 10.1182/blood-2004-08-2976.

Reprints: Takeshi Inukai, Department of Pediatrics, School of Medicine, University of Yamanashi, 1110 Shimokato, Tamaho-cho, Nakakoma-gun, Yamanashi 409-3898, Japan. e-mail: tinukai@yamanashi.ac.jp

The publication costs of this article were defrayed in part by page charge payment. Therefore, and solely to indicate this fact, this article is hereby marked "advertisement" in accordance with 18 U.S.C. section 1734.

hematopoietic progenitors and, moreover, enforced expression of HLF in cytokine-dependent cells failed to inhibit apoptosis.[18,19] We then identified a bZIP factor, E4 promoter binding protein (E4BP4)/nuclear factor regulated by IL-3 (NFIL3) (Figure 1), as a physiologic counterpart of E2A-HLF. E4BP4 has nearly identical DNA-binding specificity to CES-2 and its expression is tightly regulated by interleukin (IL-3) in IL-3–dependent cell lines such as FL5.12 and Baf-3. Moreover, enforced expression of E4BP4 delays apoptosis of IL-3–deprived cells.[23,24] These data suggested that subversion of the roles of antiapoptotic bZIP factors normally regulated by cytokines is 1 critical aspect of leukemogenesis induced by E2A-HLF.

Other bZIP factors may also play important roles in the regulation of hematopoietic cell survival. HLF is a member of the proline- and acidic amino acid–rich (PAR) bZIP family, which also includes thyrotroph embryonic factor (TEF)[25] and albumin promoter D-box–binding protein (DBP)[26] (Figure 1). TEF was originally cloned as a factor expressed in the developing anterior pituitary gland that could *trans*-activate the *TSHβ* promoter,[25] whereas DBP was cloned as a liver-enriched transcriptional activator that binds to the D element of the albumin promoter.[26] It has been well documented that the PAR proteins as well as E4BP4 are implicated in circadian control.[27-33] PAR proteins may also be involved in the regulation of cell death because all 3 PAR proteins exhibit nearly identical DNA-binding specificity to that of E4BP4 and CES-2.[25,26,28,29,34-37] Here we demonstrate that TEF promotes the survival of FL5.12 cells due to IL-3 starvation. Unexpectedly, we also found that TEF potently represses the expression of the β subunits of the IL-3 receptor, blocking proliferation and leading to arrest of the cell cycle in the G_0/G_1 phase, even in the presence of IL-3.

Materials and methods

Constructs of eukaryotic expression vectors

Expression plasmids containing the cDNAs of wild-type *TEF* (pMT-TEF), a mutated *TEF* (pMT-TEF basic mutant [BX]), and *E2AHLF* (pMT–E2A-HLF) were constructed with the pMT-CB6$^+$ eukaryotic expression vector (a gift from F. Rauscher III, Wistar Institute, Philadelphia, PA), which contains the inserted cDNA under the control of a sheep metallothionein promoter as well as the neomycin resistance gene driven by the simian virus 40 early promoter. The cDNA encoding a basic mutant of TEF (TEF/BX) that contained substitutions for 6 of the amino acid residues in the basic region critical for DNA binding (TRRKKNNVAAK mutated to TSPKSYNVPPK; single-letter code) was made by polymerase chain reaction (PCR) mutagenesis.

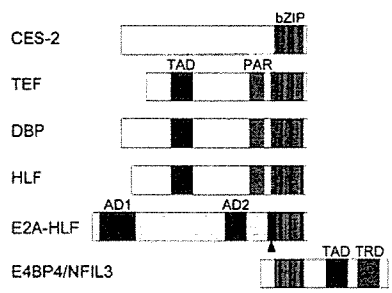

Figure 1. Schematic representation of the CES-2, TEF, DBP, HLF, E2A-HLF, and E4BP4/NFIL3 proteins. The CES-2 protein in *C elegans* contains a basic region/leucine zipper (bZIP) domain in the carboxyl-terminal region and acts as a transrepressor. TEF, DBP, and HLF contain a proline- and acidic amino acid–rich (PAR) domain as well as a bZIP domain in the carboxyl-terminal region, which shows high level of sequence identity to that of CES-2. TEF, DBP, and HLF each also contain a *trans*-activation domain (TAD) and can act as transcriptional activators. The E2A-HLF fusion protein, which is expressed in t(17;19)–positive leukemia cells, retains the 2 transactivation domains in the amino terminal of E2A (AD1 and AD2) but not its basic region/helix-loop-helix domain, which is replaced by the bZIP domain of HLF. E2A-HLF has a joining region (■ with arrowhead) generated at the breakpoint but not the basic region extension (BRE; indicated with ▤) nor the PAR domain of HLF, which contribute to sequence-specific DNA binding. E4BP4/NFIL3 contains a bZIP domain in its amino-terminal region and has nearly identical DNA-binding specificity as that of CES-2, TEF, DBP, HLF, and E2A-HLF. E4BP4 acts as either a transactivator or transrepressor depending on complexes formed by its TAD or transrepression domain (TRD) in its carboxyl-terminal region.

Cell culture and cell survival assay

FL5.12 cells, which are murine IL-3–dependent cells, were cultured in RPMI 1640 medium supplemented with 10% fetal calf serum and 0.5% 10T1/2 cell-conditioned medium as a source of IL-3. Transfectants were generated by electroporation using 2×10^7 cells and 80 μg of DNA with a gene pulser (Bio-Rad, Hercules, CA) set at 300 mV and 960 μF. Cells were then cultured in 24-well dishes and selected in the presence of the neomycin analog G418 (0.6 mg/mL) for 2 weeks. The induction of protein expression with Zn in G418-resistant cells was confirmed by immunoblot analysis. Cell growth and cell survival experiments were performed using 3 independent pools of cells, and the results of representative data of multiple experiments are shown. For cell survival assays, cells growing exponentially in IL-3–containing medium were precultured for 16 hours in the presence or absence of 100 μM $ZnSO_4$. Cells were washed with IL-3–free medium twice and were adjusted to 5×10^5 cells per milliliter. Viable cell counts were determined by trypan blue dye exclusion.

Immunoblot analysis

Cells were solubilized in Nonidet P-40 lysis buffer (150 mM NaCl, 1.0% Nonidet P-40, 50 mM Tris [tris(hydroxymethyl)aminomethane; pH 8.0]), and total cellular proteins were separated by sodium dodecyl sulfate–polyacrylamide gel electrophoresis. After wet electrotransfer onto polyvinylidene difluoride membranes, proteins were detected with the following primary antibodies: anti-HLF c-terminal (C),[35] anti-p44/42 mitogen-activated protein kinase (MAPK; New England BioLabs, Beverly, MA), anti-p70S6K (New England BioLabs), anti-Akt (New England BioLabs), antiphospho–signal transducers and activators of transcription 5 (anti–phospho-STAT5; Tyr694; New England BioLabs), anti–phospho-p44/42MAPK (Thr202/Tyr204; New England BioLabs), anti–phospho-p70S6K (Thr421/Ser424; New England BioLabs), and anti–phospho-Akt (Ser473; New England BioLabs) rabbit serum, or anti–β-tubulin (Pharmingen, San Diego, CA), antiphosphotyrosine (Upstate Biotechnology, Lake Placid, NY), and anti-STAT5 (Transduction Laboratories, Lexington, KY) mouse monoclonal antibodies. Then, the blots were stained by horseradish peroxidase–conjugated anti–rabbit or anti–mouse immunoglobulin G (IgG) and IgM secondary antibodies (MBL, Nagoya, Japan), respectively, and subjected to enhanced chemiluminescence detection (Amersham Life Science, Arlington Heights, IL).

Flow cytometric analysis

Cells (2×10^5) were washed with phosphate-buffered saline (PBS) and incubated with rat monoclonal antibodies specific for the mouse IL-3 receptor α chain (5B11)[38] or the mouse IL-3 receptor β chain (AIC2A; β_{IL3}; 9D3)[39] on ice for 30 minutes. Cells were washed with PBS and stained with a fluorescein isothiocyanate (FITC)–conjugated goat anti–rat IgG (Jackson Immuno Research Laboratories, West Grove, PA). For detection of the common β chain of the IL-3 receptor (AIC2B; β_C), cells were incubated with an anti–mouse β_C chain hamster monoclonal antibody (MBL), followed by incubation with an FITC-conjugated goat anti–hamster IgG secondary antibody (Jackson Immuno Research Laboratories). Cells were analyzed by flow cytometry (FACS Calibar; Becton Dickinson, San Jose, CA).

Northern blot analysis

Total cellular RNA was isolated by the guanidinium-cesium chloride method. RNA samples (approximately 20 μg per lane) were separated by

electrophoresis in 1% agarose gel containing 2.2 M formaldehyde, transferred to nylon membranes, and hybridized with the appropriate probes according to the standard procedure. For Northern blot analysis of multiple human hematolymphoid tissues, the blot was purchased from Clontech (Palo Alto, CA). Unique cDNA probes in the 3′ untranslated region of the PAR genes,[40] a 1.3-kilobase (kb) *Xho*I fragment of mouse IL-3 receptor α-chain cDNA, and a 0.8-kb *Xho*I/*Bam*HI fragment of mouse IL-3 receptor β_{IL3} chain cDNA were used as probes.

Analysis of gene expression in subsets of hematopoietic stem and progenitor cells

Cells (5×10^3) with surface marker expression patterns typical of hematopoietic stem cells (HSCs) and various types of myeloid and lymphoid progenitors were sorted from mouse bone marrow by fluorescence-activated cell sorting (FACS), as previously described.[41] Total RNA was prepared with TRIZOL reagent and subjected to cDNA synthesis with the SuperScript first-strand cDNA synthesis system (GIBCO, Carlsbad, CA). PCR was performed for 40 cycles of 94°C for 30 seconds, 55°C for 45 seconds, and 72°C for 45seconds with the following primers: 5′-ACCATCTTCCTCTACTGCCATCTTTCAG and 5′-GTACTTGGTCTCGTACTTGGACACGATG for first-round PCR; 5′-GTGATCTGGTTCTCCTTCAG for nested PCR amplification of *Tef:* and 5′-CACAGGACTAGAACACCTGC and 5′-GCTGGTGAAAAG-GACCTCT for PCR amplification of *Hprt*.

Electrophoretic mobility shift assay

Binding reactions in electrophoretic mobility shift assay (EMSA) were performed with a ^{32}P–end-labeled DNA oligonucleotide probe (2×10^4 counts per minute [cpm]) in 10 μL of binding buffer (12% glycerol, 12 mM HEPES [*N*-2-hydroxyethylpiperazine-*N*′-2-ethanesulfonic acid, pH 7.9], 4 mM Tris [pH 7.9], 133 mM KCl, 300 mg of bovine serum albumin per milliliter) and 5 μL of nuclear proteins extracted from FL5.12 cells by standard procedures, as previously described.[35,42] The oligonucleotide probes used were wild-type HLF consensus sequence (CS) (5′-GCTA-CATATTACGTAATAAGCGTT-3′); wild-type β-casein for STAT5 (5′-AGATTTCTAGGAATTCAATCC-3′); and mutant β-casein (5′-AGATT-TAGTTTAATTCAATCC-3′). As a carrier DNA, 1.5 μg of sheared calf thymus DNA or poly-d(I)d(C) was added to the reaction mixture testing for binding to HLF-CS or β-casein probe, respectively. The entire mixture was incubated at 30°C for 15 minutes. In the competition inhibition experiments, an approximately 100-fold molar excess of the unlabeled oligonucleotide was added to the reaction mixture. One microliter of polyvalent HLF(C) antiserum or preimmune rabbit serum was added to the nuclear lysates and incubated at 4°C for 30 minutes prior to the DNA-binding reaction. Nondenaturing polyacrylamide gels containing 4% acrylamide and 2.5% glycerol were prerun at 4°C in a high–ionic-strength Tris-glycine buffer for 30 minutes, loaded with the samples containing protein–DNA complexes, run at 35 mA for approximately 90 minutes, dried under vacuum, and analyzed by autoradiography.

Results

Expression of *TEF* in hematolymphoid tissues

The 3 members of the PAR family of proteins are differentially expressed in tissues and organs.[8,10,40] In contrast to HLF, which shows tissue-specific expression, TEF and DBP are expressed ubiquitously, although their expression in normal hematopoietic and lymphoid tissues has not been clarified. First, we performed Northern blot analysis of human hematolymphoid tissues using a specific cDNA probe. As shown in Figure 2A, *TEF* was expressed in the spleen, lymph node, thymus, and fetal liver but was nearly undetectable in peripheral blood leukocytes and bone marrow. *DBP* was widely expressed in hematolymphoid tissues, whereas *HLF* was expressed in the fetal liver alone. Second, subsets of mouse hematolymphoid progenitors were sorted from the bone marrow

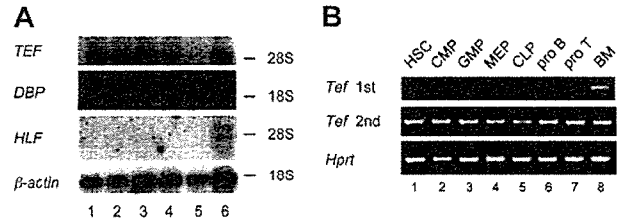

Figure 2. Expression of *TEF* during hematopoiesis. (A) Northern blot analysis of human hematolymphoid tissues. The blot was hybridized with human *TEF, DBP, HLF,* and β-actin cDNA probes. Lane 1, spleen; lane 2, lymph node; lane 3, thymus; lane 4, peripheral blood leukocyte; lane 5, bone marrow (BM); and lane 6, fetal liver. The mobility of 28S and 18S rRNA was indicated. (B) Patterns of *Tef* expression in murine myeloid and lymphoid progenitors in different stages of development. cDNA was synthesized from total RNA extracted from 5000 cells of each hematopoietic progenitor subset that had been sorted from bone marrows by FACS (lanes 1-7) as well as unpurified bone marrow mononuclear cells (lane 8). The cDNA was subjected to PCR with primers specific for the murine *Tef* (top panel) and *Hprt* (bottom panel) genes. The PCR product of amplification of *Tef* was subjected to nested PCR (middle panel). HSC indicates hematopoietic stem cells; CMP, common myeloid progenitor; GMP, granulocyte-monocyte progenitor; MEP, megakaryocyte-erythrocyte progenitor; and CLP, common lymphoid progenitor.

and were subjected to reverse transcriptase–PCR (RT-PCR) for *Tef* (Figure 2B).[22] Although *Tef* was detectable in unpurified bone marrow mononuclear cells, the RT-PCR product was virtually undetectable in each subset of progenitors (Figure 2B top panel). Upon performing nested PCR using each PCR product as a template, *Tef* was detected in each subset (Figure 2B middle panel). These results suggested that *Tef* is expressed in hematolymphoid progenitors but its expression is low or restricted to a small fraction of each subset of progenitors.

Establishment of FL5.12 cells conditionally expressing TEF

To analyze the function of TEF in hematopoietic cells, we established FL5.12 cells that inducibly expressed TEF by the addition of Zn using an expression vector (pMT-CB6$^+$) under the control of a metallothionein promoter. Immunoblot analysis using the anti-HLF(C) antibody that effectively recognizes HLF, DBP, and TEF proteins[34] revealed the induction of TEF protein in cells transfected with pMT-TEF when cultured in medium containing 100 μM Zn (Figure 3A lane 4). No endogenous or leaky expression of TEF protein was detected (Figure 3A lanes 1-3). Time course analysis revealed that protein expression of TEF was detectable within 4 hours after the addition of Zn (Figure 3B lane 2) and that it reached a plateau after 16 hours (Figure 3B lanes 4-5). The expression level of TEF was related to the concentration of Zn. Upon the addition of 75 μM Zn, the TEF expression level was approximately 20% of that induced by 100 μM Zn (Figure 3C lanes 4-5), whereas no significant induction was obtained by the addition of less than 50 μM Zn (Figure 3C lanes 2-3). We also established FL5.12 cells that conditionally expressed TEF/BX (Figure 3A lanes 5-6), which is a mutant form of TEF (see "Constructions of eukaryotic expression vectors"), or E2A-HLF (Figure 3A lanes 7 and 8). EMSA using the HLF-CS probe that contains the consensus binding sequence of the PAR proteins[17] detected specific protein-DNA complexes in nuclear extracts from cells expressing either TEF (Figure 3D lanes 3-4) or E2A-HLF (Figure 3D lanes 7-8) but not in nuclear extracts from cells expressing TEF/BX (Figure 3D lanes 5-6). The lack of DNA-binding ability of TEF/BX was not due to aberrant subcellular localization because immunofluorescence studies showed that TEF/BX was localized in the nucleus (data not shown).

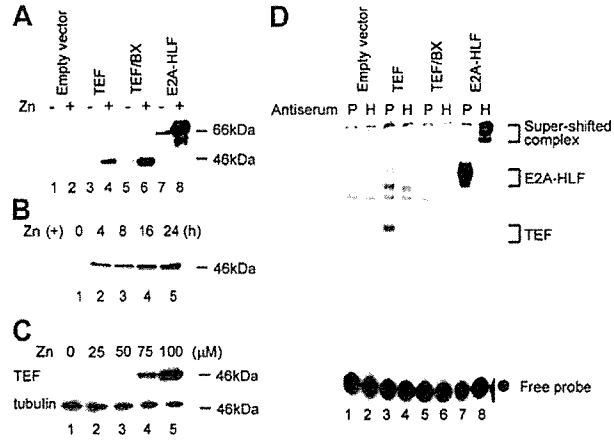

Figure 3. Establishment of FL5.12 cells conditionally expressing TEF, TEF/BX, or E2A-HLF. (A) Immunoblot analysis of FL5.12 cells using HLF(C) antiserum. Representative pools of FL5.12 cells transfected with the empty vector (lanes 1-2), pMT-TEF (lanes 3-4), pMT-TEF/BX (lanes 5-6), or pMT–E2A-HLF (lanes 7-8) were cultured in the presence (even lanes) or absence (odd lanes) of 100 μM $ZnSO_4$ for 16 hours. (B) Time course analysis of TEF expression in pMT-TEF–transfected FL5.12 cells. FL5.12 cells transfected with pMT-TEF were cultured in IL-3–containing medium in the presence of 100 μM Zn for the indicated periods of time and subjected to immunoblot analysis using the HLF(C) antiserum. (C) TEF protein expression in pMT-TEF–transfected FL5.12 cells cultured in the presence of different concentrations of Zn. FL5.12 cells transfected with pMT-TEF were cultured in the presence of Zn at the indicated concentrations for 16 hours and subjected to immunoblot analysis using the HLF(C) antiserum. The expression of tubulin was also analyzed as control. (D) Antibody-perturbed electrophoretic mobility shift analysis (EMSA) with the HLF-CS probe. FL5.12 cells transfected with the empty vector (lanes 1-2), pMT-TEF (lanes 3-4), pMT-TEF/BX (lanes 5-6), or pMT–E2A-HLF (lanes 7-8) were cultured with 100μM of Zn for 16 hours. Nuclear extracts from these cells were incubated with either preimmune (P; odd lanes) or anti-HLF(C) (H; even lanes) antiserum. Brackets show the mobility of DNA-protein complexes containing the indicated proteins and the ● indicates unbound, labeled oligonucleotide probes.

TEF but not E2A-HLF induced G_0/G_1 arrest

When TEF expression was induced by the addition of Zn in proliferating pMT-TEF–transfected FL5.12 cells cultured in IL-3–containing medium, cell growth was gradually disturbed and finally arrested within 36 hours (Figure 4A). In the dye exclusion assay, the viability of TEF-transfected cells was over 90% at 60 hours after the addition of Zn (data not shown). Growth arrest was observed when the Zn concentration was higher than 75 μM (Figure 4B). Cells transfected with pMT-TEF/BX or the empty vector proliferated exponentially in culture medium containing 100 μM Zn (Figure 4A), indicating that the growth inhibition depends on the sequence-specific DNA-binding activity of TEF and not on the cytotoxic effects of Zn. Cells transfected with pMT–E2A-HLF grew more slowly than cells transfected with the empty vector but did not undergo growth arrest (Figure 4A). Growth arrest observed in pMT-TEF–transfected FL5.12 cells was reversible after the withdrawal of Zn (Figure 4C). Cells preincubated in IL-3–containing medium in the presence of 100 μM Zn for 12 hours were washed with medium and subsequently cultured in IL-3–containing medium either in the presence or absence of 100 μM Zn. The expression of TEF was gradually decreased and became undetectable 72 hours after withdrawal of Zn (Figure 4D lanes 3, 5, 7), whereas TEF levels were maintained in the cells that were continued in culture in the presence of Zn (Figure 4D lanes 2, 4, 6). Interestingly, the growth arrest of cells cultured in the absence of Zn was reversed and cells began cycling approximately 72 hours after withdrawal of Zn, whereas the growth arrest and cell viability were maintained in the cells cultured in the presence of Zn (Figure 4C). Moreover, the growth of cells rescued by the withdrawal of Zn could be arrested again upon the subsequent readdition of Zn (Figure 4C).

To determine the cause of growth arrest, cell cycle analysis was performed using flow cytometry (Table 1). Upon the addition of Zn, TEF-expressing cells in the G_0/G_1 phase gradually accumulated and nearly 80% of the cells were in the resting phase after 48 hours. On the other hand, it was unlikely that cell death contributed to this growth arrest because the population in the sub-G_0/G_1 phase always comprised less than 10% of TEF-expressing cells (data not shown). In addition, the G_0/G_1-arrested pMT-TEF–transfected FL5.12 cells were capable of re-entering the cell cycle when Zn was withdrawn from the culture medium (Figure 4E). By contrast, in cells transfected with the empty vector, regardless of the presence or absence of Zn, more than 50% of the cells were in the S phase whereas nearly 40% of the cells were in the G_0/G_1 phase. Consistent with the slow growth rate, the number of E2A-HLF–expressing cells in the S phase slightly decreased after the addition of Zn.

TEF and E2A-HLF promoted cell survival

Next, we analyzed cell viability in the absence of IL-3 (Figure 4F). Cells were precultured in the presence or absence of Zn in IL-3–containing medium for 16 hours, washed with IL-3–free medium twice, and cultured in IL-3–free medium with or without Zn. Cells expressing E2A-HLF survived more than 72 hours in IL-3–free medium, as previously reported.[18,19] TEF also promoted cell survival in IL-3–free medium for 48 hours, but the number of viable cells gradually decreased after 72 hours even though TEF expression was maintained (data not shown). Cells expressing TEF/BX rapidly underwent apoptosis in a manner similar to that of the control cells transfected with the empty vector. These data indicated that TEF protects IL-3–dependent FL5.12 cells from apoptosis in the absence of the cytokine and that this activity depends on its DNA-binding activity.

TEF inactivated IL-3 signaling pathways

To clarify the mechanism of G_0/G_1 arrest induced by TEF, we analyzed the tyrosine phosphorylation of cellular proteins. TEF-transfected cells were preincubated in IL-3–containing medium with Zn for 18 hours, then incubated in IL-3–deficient medium with Zn for 12 hours, and then restimulated by IL-3. As previously reported by others,[43-45] rapid tyrosine phosphorylation of a wide variety of proteins was observed in cells transfected with the empty vector (Figure 5A lanes 1-4) but not in cells expressing TEF (Figure 5A lanes 5-8), suggesting that TEF inactivated signals from the IL-3 receptor. To verify the observation made in Figure 5A more precisely, we analyzed the STAT5 pathway, MAPK pathway, and phosphatidylinositol 3-kinase (PI3K) pathway by monitoring the phosphorylation status of not only STAT5[46] and p44/42 MAPK[47] but also p70S6K[48] and Akt,[49] which are downstream proteins in the PI3K pathway[47] (Figure 5B). Each FL5.12 transfectant was cultured in IL-3–free medium in the presence or absence of Zn for 12 hours following 18 hours' preincubation in IL-3–containing medium with or without Zn, respectively; subsequently exposed to IL-3 for 5 minutes; and processed for immunoblot analysis. In the absence of Zn, IL-3 stimulation of cells transfected with pMT-TEF (Figure 5B lanes 3-4) as well as cells transfected with pMT-TEF/BX (Figure 5B lanes 5-6), pMT–E2A-HLF (Figure 5B lanes 7-8), or the empty vector (Figure 5B lanes 1-2) rapidly induced the phosphorylation of STAT5. In the presence of Zn, phosphorylation of STAT5 was completely abrogated in cells

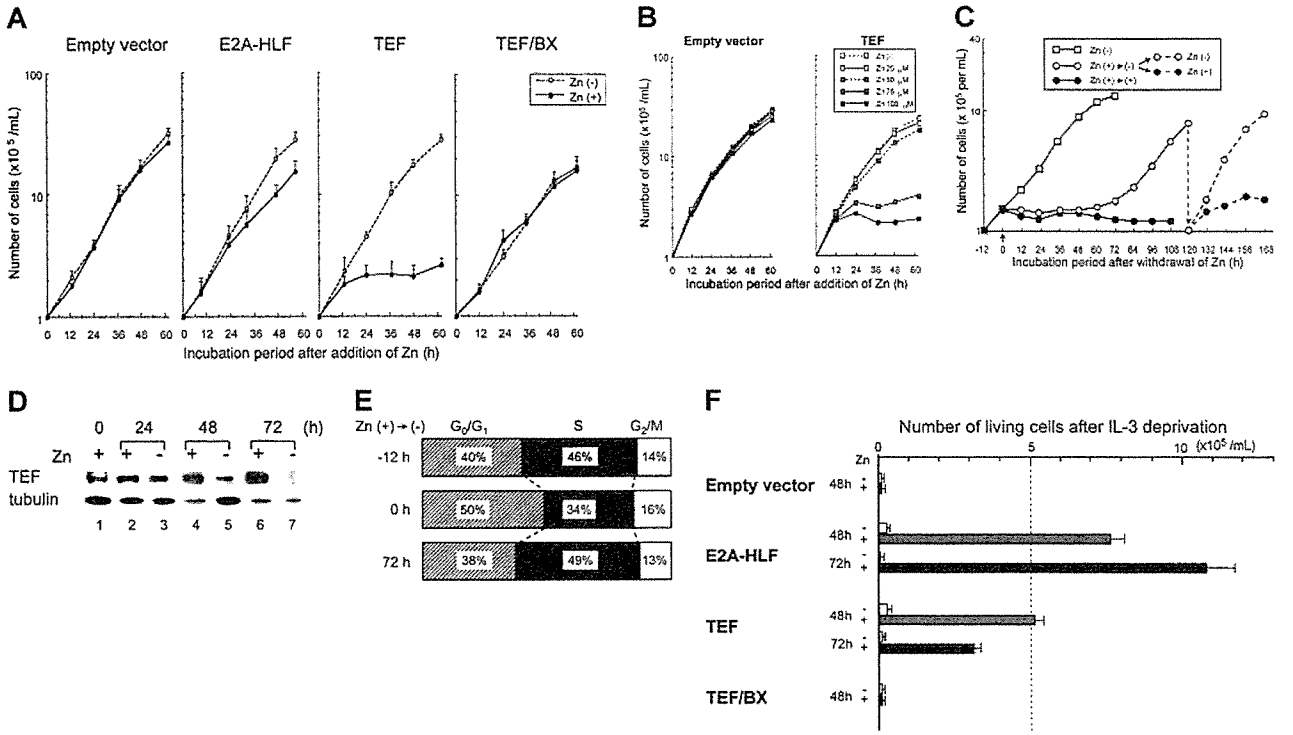

Figure 4. Growth arrest and cell survival of FL5.12 cells transfected with the TEF expression vector. (A) Growth curves of FL5.12 cells transfected with the empty vector, pMT-TEF, pMT-TEF/BX, or pMT–E2A-HLF. Cells were adjusted to 1 × 10^5 cells per mL and cultured in IL-3–containing medium in the presence (●) or absence (○) of 100 μM Zn. Representative data of multiple experiments using 3 independent pools are shown. Bars indicate standard error. (B) Growth of FL5.12 cells transfected with the empty vector or pMT-TEF in IL-3–containing medium in the presence of 0, 25, 50, 75, or 100 μM of Zn. (C) Growth curves of pMT-TEF–transfected FL5.12 cells after withdrawal of Zn. □ indicates the growth of cells cultured in IL-3–containing medium in the absence of Zn. Cells were preincubated in the presence of 100 μM Zn for 12 hours, washed with medium, adjusted to 1.5 × 10^5 cells per mL, and then cultured in IL-3–containing medium either in the presence (●) or absence (○) of 100 μM Zn. One hundred twenty hours after withdrawal of Zn, cells cultured in the absence of Zn were adjusted to 1 × 10^5 cells per mL and cultured in the presence (●- - -●) or absence (○- - -○) of 100 μM Zn. The means of triplicate samples are indicated. (D) Time course analysis of TEF expression in pMT-TEF–transfected FL5.12 cells after withdrawal of Zn. Cells were preincubated in the presence of 100 μM Zn for 12 hours, washed with medium (lane 1), then cultured in IL-3–containing medium in the presence (lanes 2, 4, and 6) or absence (lanes 3, 5, and 7) of 100 μM Zn for the indicated periods of time and subjected to immunoblot analysis using the HLF(C) antiserum. The expression of tubulin was also analyzed as control. (E) Cell cycle analysis of pMT-TEF–transfected FL5.12 cells. Cells cultured in IL-3–containing medium (top; − 12 hours) were preincubated with 100 μM of Zn for 12 hours (middle; 0 hour), washed with medium, and subsequently cultured in IL-3–containing medium in the absence of Zn for 72 hours (bottom; 72 hours). ▨ indicates G_0/G_1; ■, S; and □, G_2/M. (F) Number of viable cells after IL-3 deprivation of FL5.12 cells. FL5.12 cells transfected with the empty vector, pMT-TEF, pMT-TEF/BX, or pMT–E2A-HLF were precultured in IL-3–containing medium in the presence or absence of 100 μM of Zn for 16 hours. Cells were then washed with IL-3–free medium, adjusted to 5 × 10^5 cells per mL, and cultured without IL-3 either in the presence (▨ and ■) or absence (□) of Zn, respectively. Upon deprivation of IL-3 for 48 or 72 hours, the numbers of viable cells as determined by trypan-blue dye exclusion are indicated. The mean data of 3 independent experiments are shown. Bars indicate standard error.

transfected with the TEF expression vector (Figure 5B lanes 11-12), whereas it was rapidly induced in the other transfectants (Figure 5B lanes 9-10 and 13-16). The same results were observed with regard to the phosphorylation of p44/42 MAPK, p70S6K, and Akt. These results indicated that TEF, acting through its DNA-binding activity, blocked IL-3–signaling pathways whereas E2A-HLF did not. This was supported by the results of EMSA (Figure 5C), which demonstrated rapid induction of protein–DNA complexes containing STAT5 following restoration of IL-3[42] in nuclear extracts from cells transfected with the empty vector (Figure 5C lanes 1-6) but not in cells transfected with pMT-TEF (Figure 5C lanes 7-10).

TEF induces down-regulation of the IL-3 receptor β chains

The inactivation of IL-3 signaling observed in Figure 5 could be explained by down-regulation of the IL-3 receptor by TEF. In mice, the high-affinity IL-3 receptor is a heterodimer of the IL-3–specific α chain and either of the β_{IL3} chain or the β_C chain, the latter of which is shared with the IL-5 and granulocyte-macrophage

Table 1. Cell-cycle analysis of FL5.12 cells in the presence of IL-3

	Empty vector, %			TEF, %			E2A-HLF, %		
Zn+, h*	G_0/G_1	S	G_2/M	G_0/G_1	S	G_2/M	G_0/G_1	S	G_2/M
0	37	56	7	32	54	14	30	63	7
8	ND	ND	ND	39	43	17	ND	ND	ND
16	ND	ND	ND	54	27	18	ND	ND	ND
24	41	52	7	61	19	20	47	40	13
48	39	53	8	79	9	12	35	50	14

Data of representative pools of each transfectant are indicated.
ND indicates not determined.
*Hours of incubation with Zn.

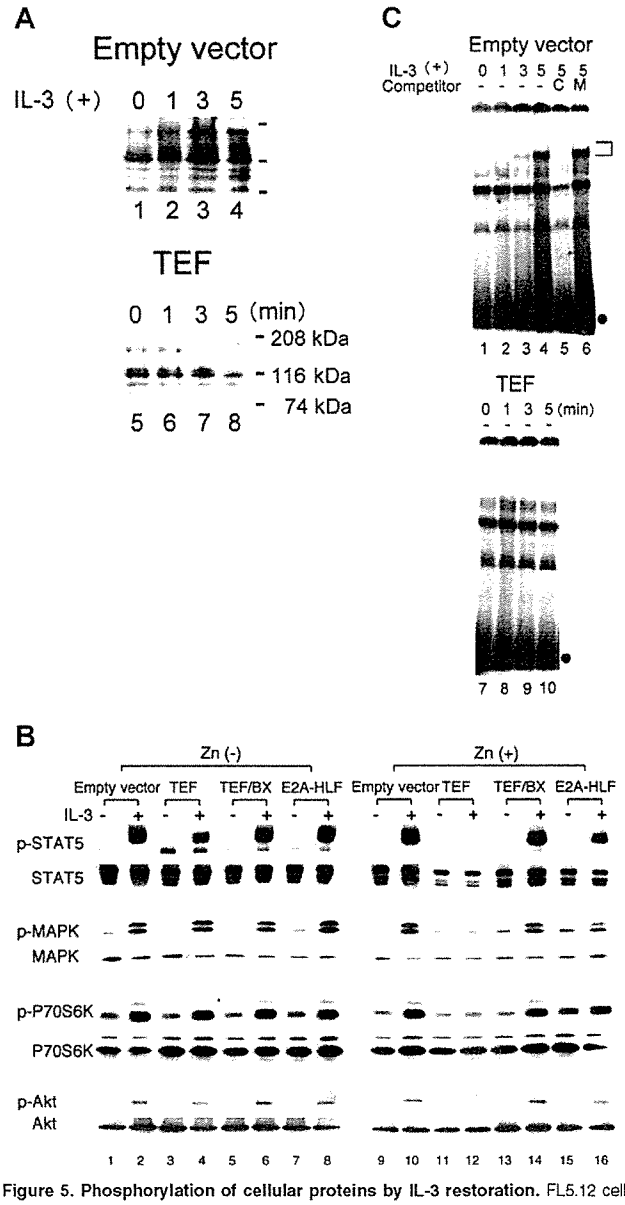

Figure 5. Phosphorylation of cellular proteins by IL-3 restoration. FL5.12 cells transfected with the empty vector, pMT-TEF, pMT-TEF/BX, or pMT–E2A-HLF were cultured in IL-3–containing medium in the presence or absence of Zn for 16 hours, and then the cells were transferred to IL-3–deficient medium in the presence or absence of Zn for 12 hours. Thereafter, cells were restimulated with IL-3 for the indicated periods of time. (A) Immunoblot analysis of FL5.12 cells that had been transfected with the empty vector (lanes 1-4) or pMT-TEF (lanes 5-8) and then cultured in IL-3–containing medium in the presence of Zn using an antiphosphotyrosine monoclonal antibody. (B) Immunoblot analysis for the phosphorylated (p) and nonphosphorylated forms of STAT5, p44/42 MAPK, p70S6K, and Akt in transfectants that had been restored with IL-3 for 5 minutes in the absence (lanes 1-8) or the presence (lanes 9-16) of Zn. The blots were probed with antiphospho-STAT5, antiphospho-p44/42 MAPK, antiphospho-p70 S6K, and antiphospho-Akt as well as anti-STAT5, anti-p44/42 MAPK, anti-p70S6K, and anti-Akt antibodies. (C) Activation of STAT5 DNA-binding by IL-3 restoration. EMSA was performed using nuclear lysates from FL5.12 cells that had been transfected with either the empty vector (lanes 1-6) or pMT-TEF (lanes 7-10) with a β-casein sequence as a probe. In the competition inhibition, an approximately 100-fold molar excess of the unlabeled β-casein sequence oligonucleotide (C; lane 5) or β-casein sequence oligonucleotide with mismatches (M; lane 6) was added in the reaction mixture. A bracket indicates the mobility of specific DNA-protein complexes and ● indicates unbound, labeled oligonucleotide probes.

colony-stimulating factor (GM-CSF) receptors.[50] Northern blot analysis was performed using an α-chain cDNA probe and a β_{IL3} chain cDNA probe; the latter recognizes both the β_{IL3} and β_C transcripts because of their extremely high levels of sequence identity (Figure 6A).[51] Upon the addition of Zn to TEF-transfected cells, the mRNA level of the β chains rapidly decreased and was almost undetectable within 16 hours. In contrast, the addition of Zn to cells transfected with either the empty vector or pMT-TEF did not change the expression level of α-chain mRNA.

Next, we analyzed the cell surface expression of the β_{IL3}, β_C, and α chains of the IL-3 receptor by flow cytometry using specific antibodies for each chain (Figure 6B). Consistent with the results of Northern blot analysis, within 24 hours after the addition of Zn, nearly complete down-regulation of the expression of both the β_{IL3} and β_C chains was observed in cells transfected with pMT-TEF but not in cells transfected with the empty vector, pMT–E2A-HLF, or pMT-TEF/BX. These data indicated that TEF down-regulates expression of the β chains in a DNA-binding–dependent fashion. Moreover, we found up-regulation of the expression of the α chain in TEF-expressing cells but not in cells transfected with the empty vector, pMT-TEF/BX, or pMT-E2A-HLF. Since Northern blot

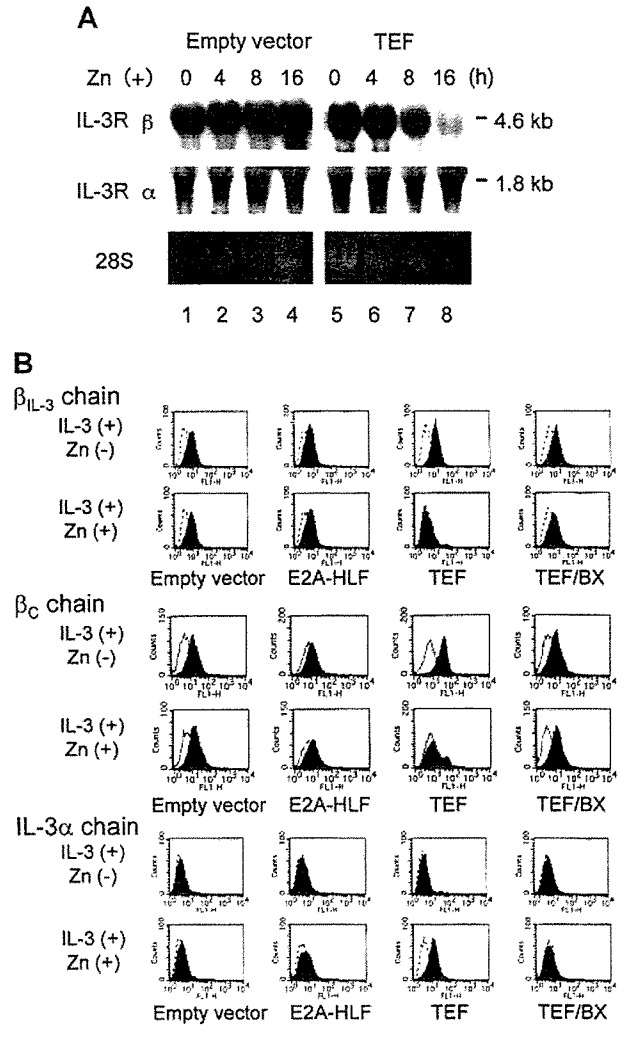

Figure 6. Northern blot analysis and flow cytometric analysis of FL5.12 cells. (A) Northern blot analysis for the IL-3 receptor. Total RNA was extracted from FL5.12 cells that had been transfected with the empty vector (lanes 1-4) or pMT-TEF (lanes 5-8) and cultured in the presence of IL-3 with Zn for the indicated periods of time. The blot was hybridized with mouse cDNA probes specific for IL-3 receptor β chains and α chain. The 28S rRNA visualized with ethidium bromide staining is shown in the bottom panel. (B) Flow cytometric analysis for surface expression of the IL-3 receptor. FL5.12 cells transfected with the empty vector, pMT–E2A-HLF, pMT-TEF, or pMT-TEF/BX were cultured in IL-3–containing medium in the presence or absence of Zn for 24 hours. Cells were analyzed with the specific antibodies for mouse β_{IL3}, β_C, or α chains. Dotted or solid lines indicate the histograms of control staining, and filled curves indicate those of specific antibodies.

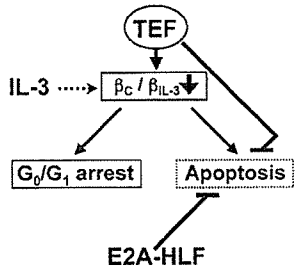

Figure 7. Hypothetical roles of TEF and E2A-HLF. TEF down-regulates the expression of the common β (β_C) chain and inactivates IL-3 signaling pathways, which are critical for both cell proliferation and cell survival. In addition, TEF promotes cell survival in the absence of survival signalings downstream of IL-3. Consequently, cells in the G_0/G_1 phase accumulated without undergoing apoptosis. In contrast, E2A-HLF blocks apoptosis without regulating the expression of cytokine receptors.

analysis revealed that the level of mRNA expression of the α chain did not change (Figure 6A), up-regulation of the cell surface α-chain expression by TEF was due to posttranscriptional mechanism(s), probably inhibition of internalization caused by down-regulation of the expression of β chains.[52] These observations indicated that TEF disrupts formation of the IL-3 receptor by down-regulating the cell surface expression of the β chains, thus rendering FL5.12 cells insensitive to IL-3.

Discussion

In this study, using a Zn-inducible system, TEF protein expression was induced in pMT-TEF–transfected FL5.12 cells within 4 hours after the addition of Zn (Figure 3B). The mRNA expression levels of the β subunits of the IL-3 receptor were reduced and became barely detectable within 16 hours (Figure 6A), and surface expression of the β chains was almost completely down-regulated within 24 hours (Figure 6B). Subsequently, the IL-3 signaling pathways were lost (Figure 5) and cells underwent cell cycle arrest in G_0/G_1 phase within 36 hours (Figure 4A; Table 1). However, the cells did not undergo apoptosis (Figure 4A) because TEF protected FL5.12 cells from apoptosis induced by IL-3 deprivation (Figure 4F). Thus, TEF induced FL5.12 cells to remain in a resting state, either in the presence or absence of IL-3 (Figure 7). These unique functions of TEF depended on its DNA-binding potential because a TEF mutant with amino acid substitutions in its basic region (TEF-BX) completely lost these activities (Figures 4-6). However, there is no potential binding site for TEF in the promoter regions of the 2 β-chain genes in the mouse[51,53] and TEF is known as a transcriptional activator.[29,37] Thus, TEF likely down-regulates transcription of the β-chain genes indirectly.

The β_C chain is common to the receptors of a series of major cytokines including IL-5 and GM-CSF as well as IL-3 and is expressed by the majority of hematopoietic progenitors (H.I. and A.K., unpublished observation, May 2004; Militi et al[54]), which expand in response to multiple growth factors during normal hematopoiesis. Therefore, it is reasonable that the *Tef* expression level in each hematolymphoid progenitor was low (Figure 2B). TEF expression may be restricted to a small fraction of progenitors that are in the resting phase and do not express the β_C chain. TEF might play an important role in preventing the exhaustion of hematopoietic progenitors by rendering a portion of the progenitors to be insensitive to growth factors. Establishment of Tef-deficient mice and extensive analysis of their hematopoiesis would elucidate the biologic significance of this unique transcription factor that regulates both cell survival and expression of cytokine receptors in hematopoietic progenitors.

This study also provides insights into functional differences between oncogenic chimeras and their normal counterparts. Similar to TEF, the E2A-HLF chimera inhibited apoptosis caused by IL-3 deprivation (Figure 4F; Inaba et al,[18] Inukai et al,[19] Altura et al[20]). However, unlike TEF, E2A-HLF did not down-regulate the expression of β subunits of the IL-3 receptor. As a result, cells expressing E2A-HLF proliferated in the presence of IL-3 (Figure 4A) and survived in the absence of IL-3 (Figure 4F). These findings suggest that the chimeric transcription factor retains the ability to drive leukemic transformation with maximum efficiency by disrupting multiple transcriptional networks. Since TEF and HLF share a high degree of sequence identity in their bZIP domains, the difference in the ability to regulate the levels of growth factor receptors between TEF and E2A-HLF is most likely caused by differences in their *trans*-activation domains (Figure 1). Alternatively, subtle changes in their DNA-binding specificity might contribute to the loss of activity of E2A-HLF to regulate cytokine receptors. The DNA-binding specificity of the PAR bZIP transcription factors is reported to be influenced by the sequences flanking the basic region, such as the basic region extension (BRE), fork region, and PAR domains.[36] Because the BRE and PAR domains of HLF are not included in the E2A-HLF chimera (Figure 1), the DNA-binding potential of E2A-HLF to suboptimal sites is substantially impaired.[34]

The antiapoptotic potential of TEF that depends on its DNA-binding activity supports a model that the consensus binding sequence recognized by the PAR factors as well as E2A-HLF, E4BP4, and CES-2 could serve as a regulatory switch for programmed cell death.[18-20,23,24] However, the detailed downstream pathways in mammalian systems have not yet been elucidated. In *C elegans*, CES-2 appears to down-regulate CES-1 expression.[5,6] Although we previously identified the *SLUG* gene, a mammalian homologue of CES-1, as one of the downstream responders of E2A-HLF in human leukemia cells with t(17;19) translocation,[23] neither TEF nor E2A-HLF was able to induce its expression in FL5.12 cells (data not shown). Thus, there must be other critical downstream pathway(s) for the antiapoptotic potential of TEF and E2A-HLF. Identification of downstream pathway(s) of TEF for its antiapoptotic potential and β_{IL3} and β_C chain gene regulation will be critical for clarifying transcriptional regulation driving normal hematopoiesis as well as leukemogenesis by E2A-HLF.

Acknowledgments

We are indebted to Dr F. Rauscher III for providing the pMT-CB6+ Zn inducible vector. This research was supported by grants-in-aid from the Ministry of Education, Science and Culture of Japan.

References

1. Horvitz HR, Shahan S, Hengarter MO. The genetics of programmed cell death in the nematode *Caenorhabditis elegans*. Cold Spring Harb Symp Quant Biol. 1994;59:377-385.
2. Ellis RE, Horvitz HR. Two *C. elegans* genes control the programmed deaths of specific cells in the pharynx. Development. 1991;112:591-603.
3. Metzstein M, Hengartner M, Tsung N, Ellis R, Horvitz HR. Transcriptional regulator of programmed cell death encoded by *Caenorhabditis elegans* gene *ces-2*. Nature. 1996;382:545-547.
4. Metzstein M, Horvitz HR. The *C. elegans* cell death specification gene ces-1 encodes a Snail family Zn finger protein. Mol Cell. 1999;4:309-319.

5. Conradt B, Horvitz HR. The *C. elegans* protein EGL-1 is required for programmed cell death and interacts with the Bcl-2-like protein CED-9. Cell. 1998;93:519-529.
6. Jacobson MD. Programmed cell death: a missing link is found. Trends In Cell Biol. 1997;7:467-469.
7. Thellmann M, Hatzold J, Conradt B. The Snail-like CES-1 protein of *C. elegans* can block the expression of the *BH3-only* cell-death activator gene *egl-1* by antagonizing the function of bHLH proteins. Development. 2003;130:4057-4071.
8. Hunger S, Ohyashiki K, Toyama K, Cleary M. Hlf, a novel hepatic bZIP protein, shows altered DNA-binding properties following fusion to E2A in t(17; 19) acute lymphoblastic leukemia. Genes Dev. 1992;6:1608-1620.
9. Hunger S. Chromosomal translocation involving the *E2A* gene in acute lymphoblastic leukemia: clinical features and molecular pathogenesis. Blood. 1996;87:1211-1224.
10. Inaba T, Roberts M, Shapiro L, et al. Fusion of the leucine zipper gene *HLF* to the *E2A* gene in human acute B-lineage leukemia. Science. 1992; 257:531-534.
11. Yoshihara T, Inaba T, Shapiro L, Kato J, Look AT. E2A-HLF-mediated cell transformation requires both the transactivation domains of E2A and the leucine zipper dimerization domain of HLF. Mol Cell Biol. 1995;15:3247-3255.
12. Inukai T, Inaba T, Yoshihara T, Look AT. Cell transformation mediated by homodimeric E2A-HLF transcription factors. Mol Cell Biol. 1997;17:1417-1424.
13. Matsunaga T, Inaba T, Matsui H, et al. Regulation of annexin II by cytokine-initiated signaling pathways and E2A-HLF oncoprotein. Blood. 2004; 103:3185-3191.
14. Kurosawa H, Goi K, Inukai T, et al. Two candidate downstream target genes for E2A-HLF. Blood. 1999;93:321-332.
15. Dang J, Inukai T, Kurosawa H, et al. The-E2A-HLF oncoprotein activates groucho-related genes and suppresses runx1. Mol Cell Biol. 2001;21: 5935-5945.
16. Honda H, Inaba T, Suzuki T, et al. Expression of E2A-HLF chimeric protein induced T-cell apoptosis, B-cell maturation arrest, and development of acute lymphoblastic leukemia. Blood. 1999;93: 2780-2790.
17. Smith KS, Rhee JW, Naumovski L, Cleary ML. Disrupted differentiation and oncogenic transformation of lymphoid progenitors in E2A-HLF transgenic mice. Mol Cell Biol. 1999;19:4443-4451.
18. Inaba T, Inukai T, Yoshihara T, et al. Reversal of apoptosis by the leukaemia-associated E2A-HLF chimeric transcriptional factor. Nature. 1996;382: 541-544.
19. Inukai T, Inaba T, Ikushima S, Look AT. Antiapoptotic role of the AD1 and AD2 transactivation domains of E2A in pro-B lymphocytes deprived of growth factor. Mol Cell Biol. 1998;18:6035-6043.
20. Altura R, Inukai T, Ashmun R, et al. The chimeric E2A-HLF transcription factor abrogates p53-induced apoptosis in myeloid leukemia cells. Blood. 1998;92:1397-1405.
21. Inukai T, Inoue A, Kurosawa H, et al. *SLUG*, a *ces-1*-related Zn-finger transcription factor gene with antiapoptotic activity, is a downstream target of the E2A-HLF oncoprotein. Mol Cell. 1999;4: 343-352.
22. Inoue A, Seidel MG, Wu W, et al. Slug, a highly conserved zinc finger transcriptional repressor, protects hematopoietic progenitor cells from radiation-induced apoptosis in vivo. Cancer Cell. 2002;2:279-288.
23. Ikushima S, Inukai T, Inaba T, et al. Pivotal role of the NFIL3/E4BP4 transcription factor in interleukin 3-mediated survival of pro-B lymphocytes. Proc Natl Acad Sci U S A. 1997;94:2609-2614.
24. Kuribara R, Kinoshita T, Miyajima A, et al. Two distinct interleukin-3-mediated signal pathways, Ras-NFIL3 (E4BP4) and Bcl-x_L, regulate the survival of murine pro-B lymphocytes. Mol Cell Biol. 1999;19:2754-2767.
25. Drolet D, Scully K, Simmons D, et al. TEF, a transcription factor expressed specifically in the anterior pituitary during embryogenesis, defines a new class of leucine zipper proteins. Genes Dev. 1991;5:1739-1753.
26. Mueller CR, Maire P, Schibler U. DBP, a liver-enriched transcriptional activator, is expressed late in ontogeny and its tissue specificity is determined posttranscriptionally. Cell. 1990;61:279-291.
27. Wuarin J, Schibler U. Expression of the liver-enriched transcriptional activator protein DBP follows a stringent circadian rhythm. Cell. 1990;63: 1257-1266.
28. Falvey E, Fleury-Olela F, Schibler U. The rat hepatic leukemia factor (HLF) gene encodes two transcriptional activators with distinct circadian rhythms, tissue distributions and target preferences. EMBO J. 1995;14:4307-4313.
29. Fonjallaz P, Ossipow V, Wanner G, Schibler U. The two PAR leucine zipper proteins, TEF and DBP, display similar circadian and tissue-specific expression, but have different target promoter preferences. EMBO J. 1996;15:351-362.
30. Lopez-Molina L, Conquet F, Dubois-Dauphin M, Schibler U. The DBP gene is expressed according to a circadian rhythm in the suprachiasmatic nucleus and influences circadian behavior. EMBO J. 1997;16:6762-6771.
31. Balsalobre A, Damiola F, Schibler U. A serum shock induces circadian gene expression in mammalian tissue culture cells. Cell. 1998;93: 929-937.
32. Yamaguchi S, Mitsui S, Yan L, et al. Role of DBP in the circadian oscillatory mechanism. Mol Cell Biol. 2000;20:4773-4781.
33. Mitsui S, Yamaguchi S, Matsuo T, Ishida Y, Okamura H. Antagonistic role of E4BP4 and PAR proteins in the circadian oscillatory mechanism. Genes Dev. 2001;15:995-1006.
34. Hunger S, Brown R, Cleary M. DNA-binding and transcriptional regulatory properties of hepatic leukemia factor (HLF) and the t(17;19) acute lymphoblastic leukemia chimera E2A-HLF. Mol Cell Biol. 1994;14:5986-5996.
35. Inaba T, Shapiro L, Funabiki T, et al. DNA-binding specificity and trans-activating potential of the leukemia-associated E2A-hepatic leukemia factor fusion protein. Mol Cell Biol. 1994;14:3403-3413.
36. Haas N, Cantwell C, Johnson P, Burch J. DNA-binding specificity of the PAR basic leucine zipper protein VBP partially overlaps those of the C/EBP and CREB/ATF families and is influenced by domains that flank the core basic region. Mol Cell Biol. 1995;15:1923-1932.
37. Hunger S, Li S, Fall M, Naumovski L, Cleary M. The proto-oncogene HLF and the related basic leucine zipper protein TEF display highly similar DNA-binding and transcriptional regulatory properties. Blood. 1996;87:4607-4617.
38. Hara T, Miyajima A. Two distinct functional high affinity receptors for mouse interleukin-3 (IL-3). EMBO J. 1992;11:1875-1884.
39. Ogorochi T, Hara T, Wang H, Maruyama K, Miyajima A. Monoclonal antibodies specific for low-affinity interleukin-3 (IL-3) binding protein AIC2A: evidence that AIC2A is a component of a high-affinity IL-3 receptor. Blood. 1992;79:895-903.
40. Khatib Z, Inaba T, Valentine M, Look AT. Chromosomal localization and cDNA cloning of the human DBP and TEF genes. Genomics. 1994;23: 344-351.
41. Akashi K, Traver D, Miyamoto T, Weissman IL. A clonogenic common myeloid progenitor that give rise to all myeloid lineages. Nature. 2000;404: 193-197.
42. Mui A, Wakao H, O'Farrell A, Harada N, Miyajima A. Interleukin-3, granulocyte-macrophage colony stimulating factor and interleukin-5 transduce signals through two STAT5 homologs. EMBO J. 1995; 14:1166-1175.
43. Isfort R, Huhn R, Frackelton A, Ihle J. Stimulation of factor-dependent myeloid cell lines with interleukin 3 induces tyrosine phosphorylation of several cellular substrates. J Biol Chem. 1988;35: 19203-19209.
44. Duronio V, Clark-Lewis I, Federsppiel B, Wieler J, Schrader J. Tyrosine phosphorylation of receptor beta subunits and common substrates in response to interleukin-3 and granulocyte-macrophage colony-stimulating factor. J Biol Chem. 1992;30:21856-21863.
45. Silvennoinen O, Witthuhn B, Quelle F, Cleveland J, Ihle J. Structure of the murine Jak2 protein-tyrosine kinase and its role in interleukin 3 signal transduction. Proc Natl Acad Sci U S A. 1993;90: 8429-8433.
46. Dumon S, Santos SC, Debierre-Grockiego F, et al. IL-3 dependent regulation of Bcl-xL gene expression by STAT5 in a bone marrow derived cell line. Oncogene. 1999;18:4191-4199.
47. Kinoshita T, Miyajima A. Raf/MAPK and rapamycin-sensitive pathway mediate the anti-apoptotic function of p21Ras in IL-3-dependent hematopoietic cells. Oncogene. 1997;15:619-627.
48. Reif K, Burgering B, Cantrell D. Phosphatidylinositol 3-kinase links the interleukin-2 receptor to protein kinase B and p70 S6 kinase. J Biol Chem. 1997;272:14426-14433.
49. Dudek H, Datta SR, Franke TF, et al. Regulation of neuronal survival by the serine-threonine protein kinase Akt. Science. 1997;275:661-665.
50. Miyajima A, Mui AL, Ogorochi T, Sakamaki K. Receptor for granulocyte-macrophage colony-stimulating factor, interleukin-3, and interleukin-5. Blood. 1993;82:1960-1974.
51. Gorman D, Itoh N, Jenkins N, et al. Chromosomal localization and organization of the murine genes encoding the β subunits (AIC2A and AIC2B) of the interleukin 3, granulocyte/macrophage colony-stimulating factor, and interleukin 5 receptors. J Biol Chem. 1992;22:15842-15848.
52. Algate P, Steelman L, Mayo M, Miyajima A, McCubrey J. Regulation of the interleukin-3 (IL-3) receptor by IL-3 in the fetal liver-derived FL5.12 cell line. Blood. 1994;83:2459-2468.
53. van Dijk T, Baltus B, Caldenhoven E, et al. Cloning and characterization of the human interleukin-3 (IL-3)/IL-5/granulocyte-macrophage colony-stimulating factor receptor βc gene: regulation by Ets family members. Blood. 1998;92:3636-3646.
54. Militi S, Riccioni R, Parolini I, et al. Expression of interleukin 3 and granulocyte-macrophage colony-stimulating factor receptor common chain β_C, β_{IT} in normal hematopoiesis: lineage specificity and proliferation-independent induction. Br J Hematol. 2000;111:441-451.

Gene Therapy (2005) 12, 203–210

www.nature.com/gt

RESEARCH ARTICLE

Efficient and stable Sendai virus-mediated gene transfer into primate embryonic stem cells with pluripotency preserved

K Sasaki[1,2], M Inoue[3], H Shibata[1], Y Ueda[3], S-i Muramatsu[4], T Okada[1], M Hasegawa[3], K Ozawa[1] and Y Hanazono[1]

[1]*Center for Molecular Medicine, Jichi Medical School, Minamikawachi, Tochigi, Japan;* [2]*Department of Plastic and Reconstructive Surgery, Faculty of Medicine, University of Tokyo, Bunkyo-ku, Tokyo, Japan;* [3]*DNAVEC Corporation, Tsukuba, Ibaraki, Japan; and* [4]*Department of Neurology, Jichi Medical School, Minamikawachi, Tochigi, Japan*

Efficient gene transfer and regulated transgene expression in primate embryonic stem (ES) cells are highly desirable for future applications of the cells. In the present study, we have examined using the nonintegrating Sendai virus (SeV) vector to introduce the green fluorescent protein (GFP) gene into non-human primate cynomolgus ES cells. The GFP gene was vigorously and stably expressed in the cynomolgus ES cells for a year. The cells were able to form fluorescent teratomas when transplanted into immunodeficient mice. They were also able to differentiate into fluorescent embryoid bodies, neurons, and mature blood cells. In addition, the GFP expression levels were reduced dose-dependently by the addition of an anti-RNA virus drug, ribavirin, to the culture. Thus, SeV vector will be a useful tool for efficient gene transfer into primate ES cells and the method of using antiviral drugs should allow further investigation for regulated SeV-mediated gene expression.
Gene Therapy (2005) **12,** 203–210. doi:10.1038/sj.gt.3302409
Published online 14 October 2004

Keywords: *primate embryonic stem cell; Sendai virus vector; gene transfer; green fluorescent protein; pluripotency; ribavirin*

Introduction

Since human embryonic stem (ES) cell lines have the ability to both proliferate indefinitely and differentiate into multiple tissue cells,[1,2] they are expected to have clinical applications as well as to serve as models for basic research and drug development. Although efficient and stable gene transfer into primate ES cells would be useful for such purposes, it has been difficult and only lentiviral vectors have been successful in achieving it.[3–5] We have previously developed Sendai virus (SeV) vectors that replicate in the form of negative-sense single-stranded RNA in the cytoplasm of infected cells and do not go through a DNA phase.[6] SeV vectors can efficiently introduce foreign genes without toxicity into airway epithelial cells,[7] vascular tissue,[8] skeletal muscle,[9] synovial cells,[10] retinal tissue,[11] and hematopoietic progenitor cells.[12] Here we report that the SeV-mediated gene transfer into primate ES cells is very efficient and stable even after the terminal differentiation of the cells. In addition, we show that SeV-mediated transgene expression levels can be reduced by the addition of a ribonucleoside analog, ribavirin, to the culture. Ribavirin is a mutagen and inhibitor of viral RNA polymerase.[13,14] It shows antiviral activity against a variety of RNA viruses and is used to treat infections of hepatitis C virus in combination with interferon-α[15,16] and of lassa fever virus.[17] The method of using antiviral drugs might offer a novel approach for regulated SeV-mediated gene expression in primate ES cells.

Correspondence: Dr Y Hanazono, Center for Molecular Medicine, Jichi Medical School, 3311-1 Yakushiji, Minamikawachi, Tochigi 329-0498, Japan
Received 20 April 2004; accepted 27 August 2004; published online 14 October 2004

Results

SeV-mediated gene transfer into ES cells

In this study, we have used an SeV vector, which is capable of self-replication but incapable of transmitting to other cells.[6] The vector does not encode the fusion (F) protein (Figure 1a), which is essential for viral entry into cells. It can be propagated only in a packaging cell line expressing the F protein. The green fluorescent protein (GFP) gene was introduced after the leader sequence of the vector genome. Cynomolgus ES cells[18] were exposed to the SeV vector for 24 h. Flow cytometric analysis at 2 days after infection showed that 15, 38, and 61% of cells fluoresced at 2, 10, and 50 transducing units (TU) per cell, respectively (Figure 1b). The gene transfer efficiency of about 60% is comparable to or even better than that for lentiviral vectors.[3] We confirmed that the undifferentiated cell fractions remained unchanged after the infection with SeV vector, as assessed by the expression of undifferentiated markers, alkaline phosphatase and SSEA-4 (data not shown). The GFP expression after infection was stable at least for a month. On the other hand, the GFP gene transfer to cynomolgus ES cells with adenovirus- and adeno-associated virus (AAV)-based vectors resulted in much lower expression levels (<20% by flow cytometry) and the levels declined to zero within a week after infection (Figure 1c).

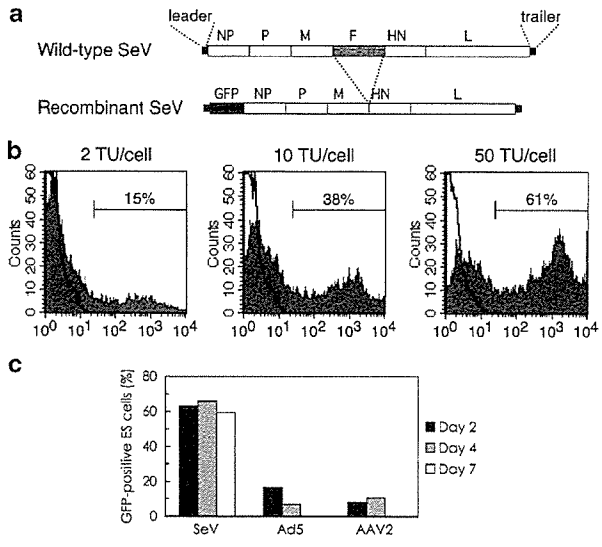

Figure 1 High-level transgene expression in cynomolgus ES cells after infection with SeV vector. (a) Schematic diagrams of the wild-type SeV genome and recombinant F-defective SeV carrying the GFP gene (SeV vector in this study). The SeV genome is 15 384 nucleotides long and its genes (NP, P, M, F, HN, and L) are in order from 3′ to 5′ in the negative-strand RNA. In the SeV vector, the entire fusion (F) gene was removed and the GFP gene was introduced at a unique NotI site between the leader sequence and NP gene. (b) The GFP expression by the SeV vector in cynomolgus ES cells. Cynomolgus ES cells were infected with the SeV vector at 2, 10, and 50 TU/cell. The flow cytometric profiles at day-2 postinfection are shown in gray. The white areas indicate uninfected ES cells. The fractions of GFP-positive cells are indicated. (c) The GFP expression levels in cynomolgus ES cells infected with the SeV (50 TU/cell), adenovirus serotype 5 (Ad5, 3.4 × 10² g.c./cell), and AAV serotype 2 (AAV2, 2.4 × 10⁴ g.c./cell) vectors. The fractions of GFP-positive cells were examined by flow cytometry at 2, 4, and 7 days postinfection.

We plucked fluorescent ES cell colonies under a fluorescent microscope once at 1 month after infection and propagated them. After this selection procedure, approximately 90% of the ES cells expressed GFP (Figure 2a and b) and the high-level expression was stable for a year as assessed by flow cytometry (Figure 2c, upper). The mean fluorescence intensity per cell was also stable (Figure 2c, lower), indicating that the replicating vector genome was almost equally delivered to each cell of all progeny. The self-replication of the SeV vector in infected cells was confirmed by RNA-PCR that amplified the viral RNA genomic sequence (Figure 3a). The GFP cDNA sequence, however, could not be detected by DNA-PCR in the infected cells (Figure 3b), indicating that no DNA phase was involved in the GFP expression.

Pluripotency of infected ES cells

The SeV-infected, fluorescent cynomolgus ES cells were able to form fluorescent tumors when transplanted into immunodeficient mice (Figure 4a–c). The fluorescence was observed uniformly by fluorescent microcopy (Figure 4d and e). The tumors consisted of all three embryonic germ layer cells (Figure 4f–i). Thus, the SeV-infected ES cells were capable of forming teratomas and the SeV infection did not spoil the pluripotency of ES cells. The infected, fluorescent cynomolgus ES cells were also able to generate fluorescent embryoid bodies (Figure 5a and b), MAP-2-positive neurons (Figure 5c), clonogenic hematopoietic colonies (Figure 5d and e), and mature functional (NBT test-positive) neutrophils (Figure 5f and g), all of which fluoresced. In addition, the GFP expression levels were not decreased during the teratoma formation or differentiation, indicating that no 'silencing' of the transgene occurred.

Drug-inducible reduction of transgene expression

Next, we examined whether ribavirin inhibits the replication and transcription of the SeV vector resulting in a reduction of transgene expression. We first used a rhesus monkey kidney cell line (LLC-MK2) to test the effect of ribavirin on the replication and transcription of the SeV vector. LLC-MK2 is a standard control cell line for SeV infection. Ribavirin was added at various concentrations 2 days after the infection. The formation of viral particles quantified by the hemagglutination assay decreased drastically upon the addition of ribavirin (Figure 6a). The decrease was dependent on the dose of ribavirin. The GFP expression was also depressed dose-dependently (Figure 6b). Thus, ribavirin dose-dependently inhibits the replication and transcription of the SeV vector in LLC-MK2 cells. The toxicity associated with ribavirin was not observed in LLC-MK2 cells.

We then examined the effect of ribavirin on SeV-infected, fluorescent cynomolgus ES cells. The addition of ribavirin also resulted in a dose-dependent reduction of GFP expression in the cells (Figure 6c). Although the GFP expression was almost completely inhibited after a 3-day exposure with 4 mM of ribavirin, the cells could not be propagated thereafter. Ribavirin at high concentrations (>1 mM) hampered the proliferation of cynomolgus ES cells. With lower concentrations (0.5–0.75 mM) of ribavirin, the GFP expression level decreased by half. After the discontinuation of ribavirin treatment, the cells could be propagated and nearly regained the original level of GFP expression. The undifferentiated cell fractions were unchanged after the discontinuation as assessed by alkaline phosphatase and SSEA-4 staining (Figure 6d).

Discussion

There are several advantages in using SeV vectors over other vectors. (i) SeV vectors can infect nondividing, quiescent cells as well as dividing cells unlike oncoretroviral vectors.[7–11] Thus, they can be used to infect cells that are terminally differentiated as well as at various stages of differentiation, whether they are dividing or not. (ii) SeV vector-mediated gene transfer does not require a DNA phase. Thus, there is no concern about the unwanted integration of foreign sequences into the host genome unlike with oncoretroviral or lentiviral vectors. (iii) Transgene expression is stable even in dividing cells since the SeV vector replicates by itself in the cytoplasm of host cells. On the other hand, gene transfer using nonreplicating adenoviral and AAV vectors resulted in decreased levels of transgene expression in dividing cells over time, since the non-replicating transgene was

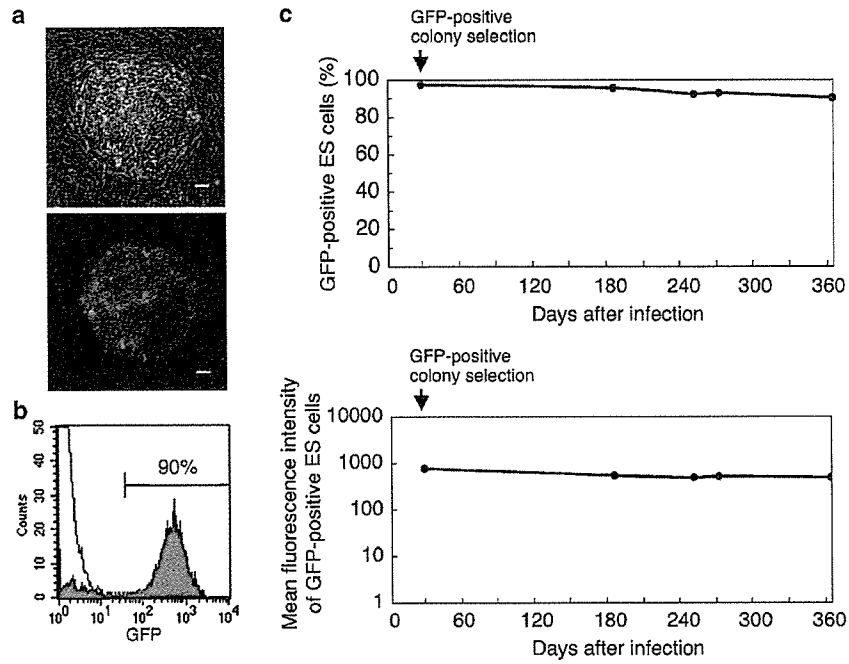

Figure 2 Stable SeV-mediated transgene expression in cynomolgus ES cells. Fluorescent ES cell colonies were plucked under a fluorescent microscope once at 1 month after infection and the cells were further propagated. (a) Phase-contrast (upper) and fluorescence (lower) images of a cynomolgus ES cell colony at day 370 after infection. Bar = 100 μm. (b) Flow cytometric analysis of SeV-infected cynomolgus ES cells at day 370 after infection (shown in green). The percentage of GFP-positive cells is indicated. Uninfected, parental cynomolgus ES cells are indicated by another line (white area). (c) The percentage of GFP-positive cells (upper) and mean fluorescence intensity per GFP-positive cell (lower) after infection with the SeV vector at 10 TU/cell are shown as a function of time (days).

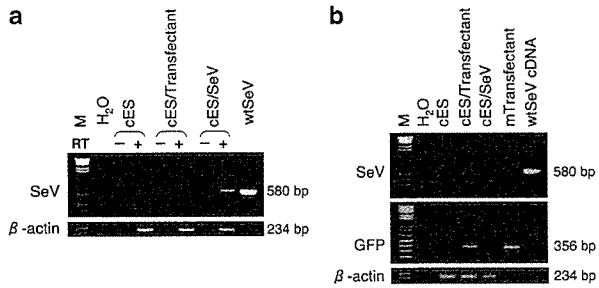

Figure 3 DNA-independent replication and transcription of SeV vector. Total cellular RNA and DNA were extracted from cynomolgus ES cells at day 284 after infection with the SeV vector. RNA-PCR (a) and DNA-PCR (b) for the SeV RNA genome or GFP sequence were conducted. The cynomolgus β-actin sequence was used as an internal control. In the RNA-PCR (a), negative results obtained without reverse transcriptase (designated RT−) confirmed that the amplified products were not derived from cellular DNA. M, 100-kb DNA ladder; cES, naive cynomolgus ES cells; cES/Transfectant, cynomolgus ES cells stably expressing the GFP gene after transfection,[33] cES/SeV, cynomolgus ES cells infected with the SeV vector; wtSeV, wild-type SeV genome; mTransfectant, a GFP-positive mouse cell line after transfection.

diluted out. (iv) The SeV vector is much less unlikely to generate wild-type virus *in vitro* or *in vivo* than oncoretroviral and lentiviral vectors, since homologous recombination between RNA genomes is very rare indeed in negative-strand RNA viruses.[19] (v) The SeV genome is not subject to cellular epigenetic modifications such as methylation, and thus it is unlikely that methylation-based silencing of transgene expression occurs.

No cytotoxic or differentiating effect on ES cells associated with the SeV infection was observed in our study. However, the wild-type SeV contains immunogenic surface proteins, hemagglutinin-neuraminidase (HN) and F proteins, which potentially induce antibody responses.[20,21] For future clinical applications, it would be desired that as many viral genes as possible are deleted from the vector backbone to permit reapplication, improve the safety, and lessen the possible toxicity of SeV vectors. To this end, we have developed a series of attenuated SeV vectors that are F gene-deleted,[6] F gene-deleted with preferable mutations,[22] M gene-deleted,[23] or have deletions of both F and M genes.[24] The modified vectors would be safer for *in vivo* use.

Ribavirin at high concentrations seems toxic to ES cells; presumably, it directly hampers viability and proliferation potential of ES cells. However, we cannot tell whether the observed toxicity is simply due to its toxicity to ES cells, as feeder cells are more highly sensitive to ribavirin than ES cells. In fact, while feeder cells died at 1 mM of ribavirin, cocultured ES cells were alive at this concentration for some time. Cynomolgus ES cells lose pluripotency and proliferation potential without feeder cells. Thus, the observed toxicity to ES cells may also be a secondary event following the injury of feeder cells. Whether the cytotoxicity is primary or secondary, it will be necessary to find modified compounds of less cytotoxicity.

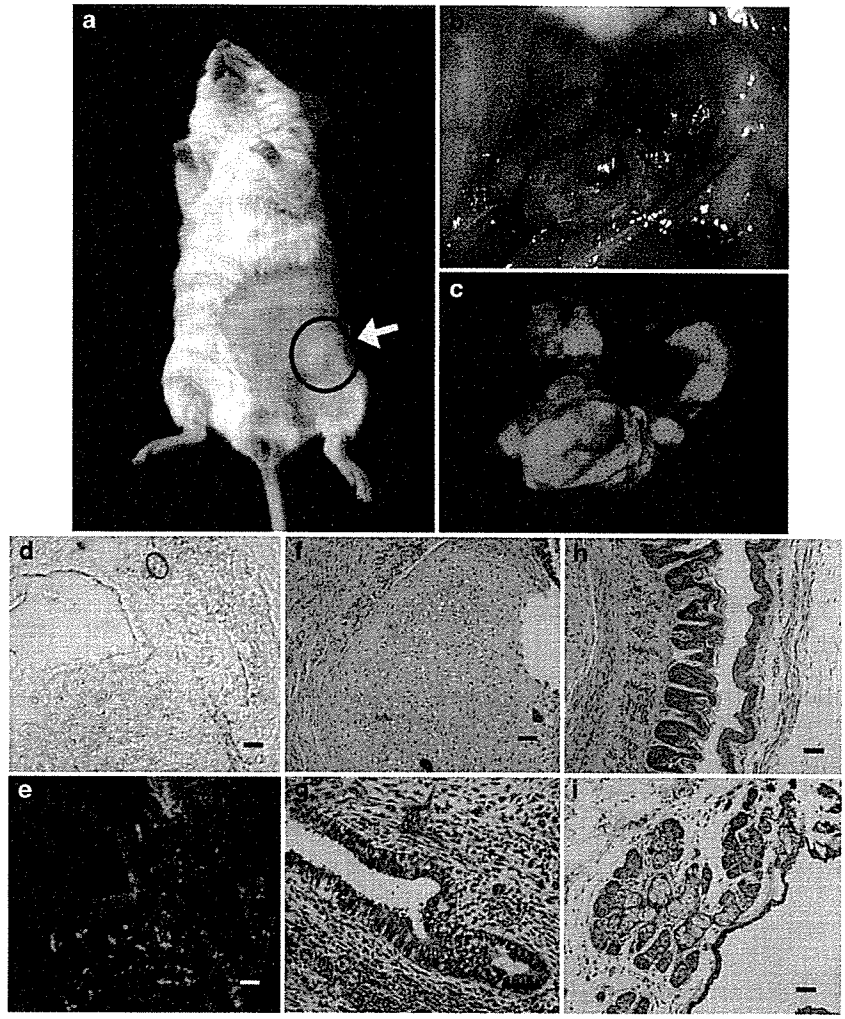

Figure 4 Pluripotency of SeV-infected cynomlgus ES cells. Tumors formed in NOD-SCID mice after inoculation of the SeV-infected cynomolgus ES cells (a). The tumor was fluorescing ((b), bright field; (c), dark field). Fluorescence was observed uniformly in the tumor under a fluorescent microscope ((d), bright field; (e), dark field). The tumor contained all three embryonic germ layer cells; cartilage (f), ciliated columnar epithelium (g), skin (h), and sebaceous gland (i) (stained with hematoxylin and eosin). Bar = 100 μm.

Materials and methods

Cell culture

Cynomolgus ES cells (CMK6) were maintained on a feeder layer of mitomycin C (Kyowa, Tokyo, Japan)-treated mouse (BALB/c) embryonic fibroblasts as described previously.[18] The culture medium consisted of Dulbecco's modified Eagle's medium (DMEM)/F12 (Invitrogen, Carlsbad, CA, USA) supplemented with 15% ES cell-qualified fetal calf serum (FCS; Invitrogen), 0.1 mM 2-mercaptoethanol (Sigma, St Louis, MO, USA), 2 mM glutamine (Invitrogen), 0.1 mM nonessential amino acids (Invitrogen), and antibiotics (100 U/ml penicillin and 100 μg/ml streptomycin, Irvine Scientific, Santa Ana, CA, USA). The ES cell colonies were routinely passaged every 3–4 days after dissociation with a combined approach of 0.25% trypsin (Invitrogen) digestion and mechanical cutting. Alkaline phosphatase staining was conducted with an Alkaline Phosphatase Chromogen Kit (Biomeda, Foster City, CA, USA). Embryoid bodies were produced by culturing ES cell aggregates in Petri dishes. LLC-MK2 cells (1×10^6) were grown in six-well plates and cultured in Eagle's minimal essential medium (Invitrogen) supplemented with 10% FCS.

Vectors

The F-defective SeV vector carrying the GFP gene was constructed as previously described.[6] The vector titer was 1.8×10^9 TU/ml determined by counting fluorescent cells after the infection of LLC-MK2 cells. Gene transfer was conducted by adding various concentrations of the SeV vector solution to culture media. After 24 h of incubation, the cells were washed twice with phosphate-buffered saline (PBS) and fresh medium was added. In some experiments, ribavirin (1-β-D-ribofuranosyl-1,2,4-triazole-3-carboxamide; Sigma) was added at various concentrations to the culture media after infection. The